

---

# DO-EM: Density Operator Expectation Maximization

---

Adit Vishnu, Abhay Shastry, Dhruva Kashyap, Chiranjib Bhattacharyya  
 Department of Computer Science and Automation  
 Indian Institute of Science, Bangalore  
 aditvishnu@iisc.ac.in

## Abstract

Density operators, quantum generalizations of probability distributions, are gaining prominence in machine learning due to their foundational role in quantum computing. Generative modeling based on density operator models (**DOMs**) is an emerging field, but existing training algorithms – such as those for the Quantum Boltzmann Machine – do not scale to real-world data, such as the MNIST dataset. The Expectation-Maximization algorithm has played a fundamental role in enabling scalable training of probabilistic latent variable models on real-world datasets. *In this paper, we develop an Expectation-Maximization framework to learn latent variable models defined through **DOMs** on classical hardware, with resources comparable to those used for probabilistic models, while scaling to real-world data.* However, designing such an algorithm is nontrivial due to the absence of a well-defined quantum analogue to conditional probability, which complicates the Expectation step. To overcome this, we reformulate the Expectation step as a quantum information projection (QIP) problem and show that the Petz Recovery Map provides a solution under sufficient conditions. Using this formulation, we introduce the Density Operator Expectation Maximization (DO-EM) algorithm – an iterative Minorant-Maximization procedure that optimizes a quantum evidence lower bound. We show that the **DO-EM** algorithm ensures non-decreasing log-likelihood across iterations for a broad class of models. Finally, we present Quantum Interleaved Deep Boltzmann Machines (**QiDBMs**), a **DOM** that can be trained with the same resources as a DBM. When trained with **DO-EM** under Contrastive Divergence, a **QiDBM** outperforms larger classical DBMs in image generation on the MNIST dataset, achieving a 40–60% reduction in the Fréchet Inception Distance.

## 1 Introduction

Recent advances in quantum hardware and hybrid quantum-classical algorithms have fueled a surge of interest in developing learning models that can operate effectively in quantum regimes [1]. Classical models rely on probability distributions; quantum systems generalize these to density operators – positive semi-definite, unit-trace operators on Hilbert spaces—that encode both classical uncertainty and quantum coherence [2]. While there is considerable progress made in quantum supervised learning, there is relatively less progress in unsupervised learning [3].

Latent variable models (LVMs) are a cornerstone of unsupervised learning, offering a principled approach to modeling complex data distributions through the introduction of unobserved or hidden variables [4]. These models facilitate the discovery of underlying structure in data and serve as the foundation for a wide range of tasks, including generative modeling, clustering, and dimensionality reduction. Classical examples such as Gaussian Mixture Models, Factor Analysis, and Hidden Markov Models [5, 6] exemplify the power of latent variable frameworks in capturing dependencies and variability in observed data. In recent years, LVMs have formed the conceptual backbone of

deep generative models including Variational Autoencoders [7], Generative Adversarial Networks [8], and Diffusion-based models [9]. The EM algorithm [10, 11] has been instrumental in deriving procedures for learning latent variables models. These algorithms are often preferred over algorithms which directly maximizes likelihood.

The study of Density Operator-based Latent Variable Models (**DO-LVM**) remains in its early stages, with foundational questions around expressivity, inference, and learning still largely unexplored [12–14]. Leveraging the modeling power of **DO-LVMs** on real-world data remains a significant challenge. Existing approaches rarely scale beyond 12 visible units—limited by restricted access to quantum hardware, the exponential cost of simulating quantum systems, and the memory bottlenecks associated with representing and optimizing **DO-LVMs** on classical devices. As a result, it is currently infeasible to empirically assess whether **DO-LVMs** offer any practical advantage on real-world datasets in terms of modeling power. EM based algorithms can provide a simpler alternative to existing learning algorithms for **DO-LVMs** which directly maximizes the likelihood. However deriving such algorithms in Density operator theoretic setup is extremely challenging for a variety of reasons, most notably there are operator theoretic inequalities, such as Jensen Inequality, which can be directly applied to derive an Evidence lower bound(ELBO) style bound for **DO-LVMs**. Precise characterization of models which are compatible with such bounds and their computational behaviour remains an important area of investigation. In this paper we bridge these research gaps by making the following contributions.

- A Density Operator Expectation-Maximization (**DO-EM**) algorithm is specified using Quantum Information Projection in Algorithm 1. **DO-EM** guarantees log-likelihood ascent in Theorem 4.4 under mild assumptions that retain a rich class of models.
- A Quantum Evidence Lower Bound (QELBO) for the log-likelihood is derived in Lemma 4.1 from a minorant-maximization perspective leveraging the Monotonicity of Relative Entropy.
- **DO-LVMs** are specialized to train on classical data in Section 5 using the **DO-EM** algorithm. This specialization we call **CQ-LVMs**, a class of models with quantum latent variables, can train real world data due to a decomposition proved in Theorem 5.1.
- Quantum-interleaved deep Boltzmann machines (Q<sub>i</sub>DBM), a quantum analog of the DBM is defined in Section 5.1. The well known Contrastive Divergence (CD) algorithm for Boltzmann machines is adapted to the Q<sub>i</sub>DBM, which when used with **DO-EM** algorithm in Section 5.1, allows Q<sub>i</sub>DBMs to be trained on MNIST-scale data.
- First empirical evidence of a modeling advantage when training **DO-LVMs** on standard computers with real-world data is provided in Section 6. Q<sub>i</sub>DBMs trained using CD on the MNIST dataset achieve a 40–60% lower Fréchet Inception Distance compared to state-of-the-art deep Boltzmann machines.

## 2 Preliminaries

**Notation** The  $\ell^2$ -norm of a column vector  $\mathbf{v}$  in a Hilbert space  $\mathcal{H}$  is given by  $\|\mathbf{v}\|_2 = \sqrt{\mathbf{v}^\dagger \mathbf{v}}$  where  $\mathbf{v}^\dagger$  denotes the conjugate transpose of  $\mathbf{v}$ . The set of Hermitian (self-adjoint) operators  $\mathcal{O} = \mathcal{O}^\dagger$  on  $\mathcal{H}$  is denoted by  $\mathfrak{L}(\mathcal{H})$ . The positive-definite subset of  $\mathfrak{L}(\mathcal{H})$  is denoted by  $\mathfrak{L}_+(\mathcal{H})$ . The Kronecker product between two operators is denoted  $A \otimes B$  and their direct sum is denoted  $A \oplus B$  [15]. The identity operator on  $\mathcal{H}$  is denoted  $I_{\mathcal{H}}$ . The null space of an operator  $A \in \mathcal{H}$  is denoted by  $\ker(A)$ .

**Latent variable models and EM algorithm** Latent Variable Models (LVMs) [4] specify the probability distribution of random variables  $V=[V_1, \dots, V_{d_V}]$  through a joint probability model

$$P(V=\mathbf{v} \mid \theta) = \sum_h P(V=\mathbf{v}, H=\mathbf{h} \mid \theta)$$

where  $H = [H_1, \dots, H_{d_L}]$  are unobserved random variables. Learning an LVM from data, a problem of great interest in Unsupervised Learning [5], refers to estimating the model parameters  $\theta$  from a dataset  $\mathcal{D} = \{\mathbf{v}^{(1)}, \dots, \mathbf{v}^{(N)}\}$  consisting of i.i.d instances drawn from the LVM. Maximum likelihood-based methods aim to maximize  $\mathcal{L}(\theta) = \frac{1}{N} \sum_{i=1}^N \ell_i(\theta)$  where  $\ell_i(\theta) = \log P(V=\mathbf{v}^{(i)} \mid \theta)$ . The maximization problem is not only intractable in most cases but even gradient-based algorithms, which

can only discover local optima, are difficult to implement because of unwieldy computations in  $\ell_i(\theta)$ . The EM algorithm [10, 11] is an alternative iterative algorithm with the scheme

$$\theta^{(k+1)} = \underset{\theta}{\operatorname{argmax}} \frac{1}{N} \sum_{i=1}^N Q_i(\theta | \theta^{(k)}), \text{ where } \ell_i(\theta) \geq Q_i(\theta | \theta^{(k)}) \text{ and } \ell_i(\theta^{(k)}) = Q_i(\theta^{(k)} | \theta^{(k)}).$$

**Boltzmann machines** Boltzmann Machines (BM) are stochastic neural networks that define a probability distribution over binary vectors based on the Ising model in statistical physics [16]. Due to the intractability of learning in fully connected BMs, the Restricted Boltzmann Machine (RBM) was introduced with no intra-layer connections, enabling efficient Gibbs sampling [17–19]. Deep Boltzmann Machines (DBM) [20] stacks RBMs using undirected connections and allow for joint training of all layers. The joint probability of a DBM with  $L$  layers,  $P(\mathbf{v}, \mathbf{h}^1, \dots, \mathbf{h}^L)$  is defined as

$$P(\mathbf{v}, \mathbf{h}_1, \dots, \mathbf{h}_{d_L}) = \frac{1}{Z} e^{-E(\mathbf{v}, \mathbf{h}_1, \dots, \mathbf{h}_{d_L})} \quad (\text{DBM})$$

where  $E(\mathbf{v}, \mathbf{h}^1, \dots, \mathbf{h}^L)$  is called the *Energy Function*, and  $Z = \sum_{\mathbf{v}, \mathbf{h}} e^{-E(\mathbf{v}, \mathbf{h}^1, \dots, \mathbf{h}^L)}$  is the *Partition Function* which is typically intractable to compute. Learning in DBMs is difficult due to intractable posterior dependencies. DBMs are usually trained using variants of the Contrastive Divergence algorithm [18, 21, 22]. A detailed discussion on Boltzmann machines and the Contrastive Divergence algorithm is provided in Appendix A.

## 2.1 Density operators

A density operator on a Hilbert space  $\mathcal{H}$  is a Hermitian, positive semi-definite operator with unit trace [2, 23]. The set of Density operators will be denoted by  $\mathcal{P}(\mathcal{H})$ , and can be regarded as generalizations of probability distributions. A joint density operator  $\rho \in \mathcal{P}(\mathcal{H}_A \otimes \mathcal{H}_B)$  can be *marginalized* to  $\rho_A \in \mathcal{P}(\mathcal{H}_A)$  by the partial trace operation  $\rho_A = \operatorname{Tr}_B(\rho) = \sum_{i=1}^{d_B} (I_A \otimes \mathbf{x}_i^\dagger) \rho (I_A \otimes \mathbf{x}_i)$  where  $\{\mathbf{x}_i\}_{i=1}^{d_B}$  is an orthonormal basis of  $\mathcal{H}_B$ . Such a  $\rho$  is *separable* if it is a convex combination of *product states*  $\rho_A \otimes \rho_B$  with  $\rho_A \in \mathcal{P}(\mathcal{H}_A)$  and  $\rho_B \in \mathcal{P}(\mathcal{H}_B)$ .

**Definition 2.1** (Umegaki [24] Relative Entropy). Let  $\omega$  and  $\rho$  be density operators in  $\mathcal{P}(\mathcal{H}_A \otimes \mathcal{H}_B)$  with  $\ker(\rho) \subseteq \ker(\omega)$ . Their relative entropy is given by  $D_U(\omega, \rho) = \operatorname{Tr}(\omega \log \omega) - \operatorname{Tr}(\omega \log \rho)$ .

Lindblad [25] showed that the relative entropy does not increase under the action of the partial trace.

**Theorem 2.2** (Monotonicity of Relative Entropy). *For density operators  $\omega$  and  $\rho$  in  $\mathcal{P}(\mathcal{H}_A \otimes \mathcal{H}_B)$  such that  $\ker(\omega) \subset \ker(\rho)$ ,  $D_U(\omega, \rho) \geq D_U(\operatorname{Tr}_B \omega, \operatorname{Tr}_B \rho)$ .*

Petz [26, 27] showed that Theorem 2.2 is saturated if and only if the Petz Recovery Map reverses the partial trace operation.

**Definition 2.3** (Petz Recovery Map). For a density operator  $\rho$  in  $\mathcal{P}(\mathcal{H}_A \otimes \mathcal{H}_B)$ , the Petz Recovery Map for the partial trace  $\mathcal{R}_\rho : \mathcal{H}_A \rightarrow \mathcal{H}_A \otimes \mathcal{H}_B$  is the map

$$\mathcal{R}_\rho(\omega) = \rho^{1/2} \left( \left( \rho_A^{-1/2} \omega \rho_A^{-1/2} \right) \otimes I_B \right) \rho^{1/2}. \quad (\text{PRM})$$

Theorem 2.2 is saturated when  $\mathcal{R}_\rho(\omega) = \omega$ . Ruskai [28] proved an equivalent condition.

**Theorem 2.4** (Ruskai’s condition). *For density operators  $\omega$  and  $\rho$  in  $\mathcal{P}(\mathcal{H}_A \otimes \mathcal{H}_B)$  such that  $\ker(\omega) \subset \ker(\rho)$ ,  $D_U(\operatorname{Tr}_B \omega, \operatorname{Tr}_B \rho) = D_U(\omega, \rho)$  if and only if  $\log \omega - \log \rho = (\operatorname{Tr}_B \omega - \operatorname{Tr}_B \rho) \otimes I_B$ .*

Ruskai’s condition can be interpreted as  $\omega$  and  $\rho$  having the same Conditional Amplitude Operator.

**Definition 2.5** (Conditional Amplitude Operator[29]). The conditional amplitude operator of a density operator  $\rho$  in  $\mathcal{P}(\mathcal{H}_A \otimes \mathcal{H}_B)$  with respect to  $\mathcal{H}_A$  is  $\rho_{B|A} = \exp(\log \rho - \log \rho_A \otimes I_B)$ .

A detailed discussion on density operators and quantum channels is provided in Appendix B.

## 3 Density operator latent variable models

In this section, we introduce Density Operator Latent Variable Models (**DO-LVM**) and recover existing models such as the Quantum Boltzmann Machine (QBM) as special cases. We discuss the computational challenges of learning such models from observations.

**Definition 3.1 (DO-LVM and the Learning Problem).** A Density Operator Latent Variable Model (**DO-LVM**) specifies the density operator  $\rho_V \in \mathcal{P}(\mathcal{H}_V)$  on observables in  $\mathcal{H}_V$  through a joint density operator  $\rho_{VL} \in \mathcal{P}(\mathcal{H}_V \otimes \mathcal{H}_L)$  as  $\rho_V = \text{Tr}_L(\rho_{VL}(\theta))$  where the space  $\mathcal{H}_L$  is not observed. Learning a **DO-LVM** is the estimation of model parameters  $\theta$  when a target density operator  $\eta_V \in \mathcal{P}(\mathcal{H}_V)$  is specified. This can be achieved by maximizing the log-likelihood

$$\mathcal{L}(\theta) = \text{Tr}(\eta_V \log \rho_V(\theta)). \quad (\text{LP})$$

*Remark 3.2.* Maximizing the log-likelihood of a **DO-LVM** is equivalent to minimizing  $D_U(\eta_V, \rho_V(\theta))$ .

We specialize **DO-LVMs** to classical datasets in Section 5.

**Hamiltonian-based models** The Hamiltonian is a Hermitian operator  $H \in \mathcal{L}(\mathcal{H})$  representing the total energy and generalizes the notion of an energy function in classical energy-based models. The model is defined using Gibbs state density matrix analogous to the Boltzmann distribution:  $\rho(\theta) = \frac{\exp(H(\theta))}{Z(\theta)}$  with  $Z(\theta) = \text{Tr} \exp(H(\theta))$  and  $H(\theta) = \sum_r \theta_r H_r$ , where  $H_r \in \mathcal{L}(\mathcal{H})$  are Hermitian operators and  $\theta_r \in \mathbb{R}$  are model parameters. The Quantum Boltzmann Machine is a Hamiltonian-based model inspired by the transverse field Ising model [12]. In this paper,  $\text{QBM}_{m,n}$  denotes a model with  $m$  visible and  $n$  hidden units with

$$H(\theta) = - \sum_{i=1}^{m+n} b_i \sigma_i^z - \sum_{i>j} w_{ij} \sigma_i^z \sigma_j^z - \sum_{i=1}^{m+n} \Gamma_i \sigma_i^x \quad (\text{QBM})$$

where  $\sigma_i^z$  and  $\sigma_i^x$  are  $2^{m+n} \times 2^{m+n}$  Pauli matrices defined by  $\sigma_i^k = \otimes_{j=1}^{i-1} \mathbf{I} \otimes \sigma^k \otimes_{j=i+1}^{m+n} \mathbf{I}$  where  $k \in \{x, z\}$ ,  $\sigma^z = \begin{pmatrix} 1 & 0 \\ 0 & -1 \end{pmatrix}$ , and  $\sigma^x = \begin{pmatrix} 0 & 1 \\ 1 & 0 \end{pmatrix}$ . A QBM is hence a **DO-LVM** with  $\rho_V(\theta) = \frac{1}{Z(\theta)} \text{Tr}_L \exp(H(\theta))$ .

Setting  $\Gamma_i = 0$  recovers the Boltzmann Machine (BM) [12]. However, the density operator representation of these classical models are plagued by their  $2^{m+n} \times 2^{m+n}$  dimensionality. The memory requirements for storing and updating models represented by density operators have been prohibitive for QBMs to scale beyond about 12 visible units.

**Need for an EM algorithm.** As probabilistic LVMs are a special case of **DO-LVMs**, the training challenges they face persist in **DO-LVMs**, which also introduce new operator-theoretic difficulties. Maximizing the log-likelihood of a **DO-LVM** involves operators that do not commute [13]. The direct computation of gradient in Equation (LP) is significantly complicated by the partial trace [30]. Due to the difficulty of working with hidden units, recent work on QBMs have focused on models without hidden units [31, 14, 32, 33]. Demidik et al. [34] studied a Restricted QBM with 12 visible units and 90 hidden units, the largest model studied in literature so far. Refer Appendix B for a detailed survey on QBM literature. Hence, training a QBM, the most popular **DO-LVM** in literature, on real-world data *remains an open challenge*.

Intractability of the gradient of the log-likelihood in probabilistic LVMs is addressed by the EM algorithm. Classical derivations of the EM algorithm fail with density operators since there is no well-defined way to construct conditional density operators [23]. An EM algorithm for density operators using Conditional Amplitude Operators (CAO) was conjectured in Warmuth and Kuzmin [35]. This is insufficient since the CAO does not provide a density operator [29]. In the next section, we appeal to well-known results in quantum information theory to derive an ELBO and EM algorithm for density operators.

## 4 The DO-EM framework

In this section, we develop an algorithmic framework applicable for learning **DO-LVMs** using a density operator expectation maximization framework.

The classical ELBO is derived for each datapoint using conditional probability and Jensen's inequality. This approach fails for density operators due to the absence well-defined quantum conditional probability [23]. In order to derive an ELBO for **DO-LVMs**, we resort to an approach inspired by the chain rule of KL-divergence [36].

**Lemma 4.1 (Quantum ELBO).** Let  $\mathcal{J}(\eta_V) = \{\eta \mid \eta \in \mathcal{P}(\mathcal{H}_V \otimes \mathcal{H}_L) \text{ \& } \text{Tr}_L \eta = \eta_V\}$  be the set of feasible extensions for a target  $\eta_V \in \mathcal{P}(\mathcal{H}_V)$ . Then for a **DO-LVM**  $\rho(\theta)$  and  $\eta \in \mathcal{J}(\eta_V)$ ,

$$\mathcal{L}(\theta) \geq \text{QELBO}(\eta, \theta) = \text{Tr}(\eta \log \rho(\theta)) + S(\eta) - S(\eta_V). \quad (\text{QELBO})$$

*Proof sketch:* We provide a proof due to Theorem 2.2 in Appendix C.

The classical EM algorithm is a consequence of the ELBO being a minorant of the log-likelihood [37, 38]. However, it is well known that Theorem 2.2 is often not saturated [39–43]. Inspired by an information geometric interpretation of the EM algorithm [44], we study an instance of a quantum information projection problem to saturate QELBO.

#### 4.1 A quantum information projection problem

In this subsection we study the  $I$ -projection [36] problem for density operators and show conditions when (PRM) can solve this problem. The problem of Quantum Information Projection (QIP) is stated as follows. Consider a density operator  $\omega$  in  $\mathcal{P}(\mathcal{H}_A)$  and a density operator  $\rho$  in  $\mathcal{P}(\mathcal{H}_A \otimes \mathcal{H}_B)$ , find  $\xi^*$  in  $\mathcal{P}(\mathcal{H}_A \otimes \mathcal{H}_B)$  such that

$$\xi^* = \underset{\text{Tr}_B(\xi)=\omega}{\text{argmin}} D_U(\xi, \rho). \quad (\text{QIP})$$

To the best of our knowledge, this problem has not been studied in literature. We know from Theorem 2.2 that the theoretical minimum attained by the objective function in QIP is  $D_U(\omega, \text{Tr}_B \rho)$  though it is not always saturated. Inspired by this connection, we explore sufficiency conditions for when PRM solves QIP.

**Definition 4.2 (Condition S).** Two density operators  $\omega$  in  $\mathcal{P}(\mathcal{H}_A)$  and  $\rho$  in  $\mathcal{P}(\mathcal{H}_A \otimes \mathcal{H}_B)$  satisfy the sufficiency condition if  $\rho$  is full rank, separable, and  $[\omega, \text{Tr}_B(\rho)] = 0$  such that  $\rho = \sum_{i=1}^{d_A} \alpha_i \mathbf{x}_i \mathbf{x}_i^\dagger \otimes \rho_B^{(i)}$  where  $\{\mathbf{x}_i\}_{i=1}^{d_A}$  is an orthonormal basis of  $\mathcal{H}_A$  and  $\rho_B^{(i)} \in \mathcal{P}(\mathcal{H}_B)$ .

**Theorem 4.3.** Suppose two density operators  $\omega$  in  $\mathcal{P}(\mathcal{H}_A)$  and  $\rho$  in  $\mathcal{P}(\mathcal{H}_A \otimes \mathcal{H}_B)$  such that **Condition S** is satisfied, the solution to the information projection problem QIP is PRM.

*Proof sketch:* The statement holds due to the fact that  $[\rho, \mathcal{R}_\rho(\omega)] = 0$  under the conditions in the theorem. Thus,  $\rho$  and  $\mathcal{R}_\rho(\omega)$  obey Ruskai’s condition. A detailed proof is provided Appendix C.

#### 4.2 DO-EM through the lens of Minorant Maximization

In this section, we present the **Density Operator Expectation Maximization (DO-EM)** algorithm from a Minorant-Maximization perspective and discuss its advantages over direct maximization of the log-likelihood. We prove that the **DO-EM** algorithm can achieve log-likelihood ascent at every iteration under **Condition S**.

For a fixed  $\theta^{(\text{old})}$ , the QELBO is maximized when  $\eta$  is the QIP of  $\rho(\theta)$  onto the set of feasible extensions. This allows us to define a potential minorant  $\mathcal{Q}$  for the log-likelihood.

$$\begin{aligned} \eta(\theta^{(\text{old})}) &= \underset{\text{Tr}_L \eta = \eta_V}{\text{argmin}} D_U(\eta, \rho(\theta^{(\text{old})})) \\ \mathcal{Q}(\theta; \theta^{(\text{old})}) &= \text{QELBO}(\eta(\theta^{(\text{old})}), \rho(\theta)) \end{aligned}$$

---

##### Algorithm 1 DO-EM

---

- 1: **Input:** Target density operator  $\eta_V$  and  $\theta^{(0)}$
  - 2: **while** not converged **do**
  - 3:   **E Step:**  $\eta^{(t)} = \underset{\eta: \text{Tr}_L \eta = \eta_V}{\text{argmin}} D_U(\eta, \rho(\theta^{(t)}))$
  - 4:   **M Step:**  $\theta^{(t+1)} = \underset{\theta}{\text{argmax}} \text{Tr}(\eta^{(t)} \log \rho(\theta))$
- 

We use  $\mathcal{Q}$  to define the **DO-EM** algorithm in Algorithm 1. Models and QIPs that obey Ruskai’s condition provably achieve log-likelihood ascent under the **DO-EM** procedure.

**Theorem 4.4** ( $\mathcal{Q}$  is a minorant). Let  $\eta_V$  be a target density matrix and  $\rho(\theta)$  be a **DO-LVM** trained by the **DO-EM** algorithm. If  $\rho(\theta^{(t)})$  and its QIP onto the set of feasible extensions,  $\eta^{(t)}$ , obey Ruskai’s condition, then  $\mathcal{Q}$  is a minorant of the log-likelihood. Then,  $\mathcal{L}(\theta^{(t+1)}) \geq \mathcal{L}(\theta^{(t)})$ , where  $\theta^{(t+1)} = \underset{\theta}{\text{argmax}} \mathcal{Q}(\theta; \theta^{(t)})$ .

*Proof sketch:* Proof using the saturation of Theorem 2.2 is in Appendix C.

**Corollary 4.5.** For a target density operator  $\eta_V$  and model  $\rho(\theta)$  satisfying **Condition S**, the E step is the Petz recovery map  $\mathcal{R}_\rho(\eta_V)$ . Moreover, such a model trained using the **DO-EM** algorithm achieves provable likelihood ascent at every iteration.

*Proof sketch:* The proof due to Theorem 4.3 and Theorem 4.4 is given in Appendix C.

The **DO-EM** algorithm can be considered a density operator analog of the classical EM algorithm. We recover the classical EM algorithm from **DO-EM** for discrete models if  $\eta_V$  and  $\rho(\theta)$  are diagonal.

The **E Step** in **DO-EM** finds a feasible extension  $\eta$  whose Conditional Amplitude Operator (CAO) is equal to that of the model  $\rho(\theta)$ . The PRM under **Condition S** is the CAO reweighted by  $\eta_V$  to give a valid density operator. This reduces to classical E step when the CAO reduces to the conditional probability and PRM reduces to Bayes rule. If the model  $\rho$  is of the form  $\rho_V \otimes \rho_L$ , we recover the conjecture in [35].

A log-likelihood involving a partial trace is often intractable. The **M Step** in **DO-EM** algorithm maximizes an expression without the partial trace. The log-likelihood of such expressions may have closed-form expressions for the gradients, for example, using the Lee-Trotter-Suzuki formula [14]. In the classical case, this is equivalent to the EM algorithm maximizing a sum of logarithms instead of a logarithm of sums.

**Corollary 4.6.** *For a Hamiltonian-based model with E step solution  $\eta^{(t)}$ , the M step reduces to*

$$\theta^{(t+1)} = \operatorname{argmax}_{\theta} \operatorname{Tr}(\eta^{(t)} H(\theta)) - \log Z(\theta)$$

*Proof sketch:* The proof due to properties of the matrix logarithm is given in Appendix C.

However, the memory footprint of **DO-LVMs** remain, preventing the application of these models on real-world data. We specialize **DO-LVMs** and **DO-EM** to train on classical data and achieve practical scale.

## 5 DO-EM for classical data

In this section, we specialize **DO-LVMs** and the **DO-EM** algorithm to classical datasets. We assume, for ease of presentation, that the data  $\mathcal{D} = \{\mathbf{v}^{(1)}, \dots, \mathbf{v}^{(N)}\}$  is sampled from the set  $\mathcal{B} = \{+1, -1\}^{d_V}$ . We consider a  $2^{d_V}$ -dimensional Hilbert space  $\mathcal{H}_V$  with standard basis  $\mathfrak{B} = \{\mathbf{v}_i\}_{i=1}^{2^{d_V}}$ . There is a one-to-one mapping between elements of  $\mathcal{B}$  and  $\mathfrak{B}$ . For any dataset  $\mathcal{D}$ , there is an equivalent dataset on  $\mathcal{H}_V$  given by  $\mathfrak{D} = \{\mathbf{v}^{(1)}, \dots, \mathbf{v}^{(N)}\}$ . The target density operator is then  $\eta_V = \frac{1}{N} \sum_{i=1}^N \mathbf{v}_i \mathbf{v}_i^\dagger$ . A **DO-LVM** on  $d_V$ -dimensional binary data is therefore a  $2^{d_V+d_L} \times 2^{d_V+d_L}$  matrix while the target  $\eta_V$  is a  $2^{d_V} \times 2^{d_V}$  matrix.

Specializing **Condition S** to diagonal target density operators, allows the decomposition of a **DO-LVM** into direct sums of smaller subspaces, making the **DO-EM** algorithm computationally easier.

**Theorem 5.1.** *If  $\rho_V$  is diagonal,  $\rho$  satisfies **Condition S** if and only if  $\rho = \oplus_i \rho_L(i)$  and  $P(\mathbf{v}_i) = \operatorname{Tr}(\rho_L(i))$  with  $\mathbf{v}_i \in \mathfrak{B}$ . The density operator for  $\mathcal{H}_L$  for a particular  $\mathbf{v}_i$  is then given by  $\frac{1}{P(\mathbf{v}_i)} \rho_L(i)$ .*

*Proof sketch:* See Appendix C.

We call models that obey Theorem 5.1 as **CQ-LVMs** since it implies a classical visible probability distribution with a quantum hidden space. QELBO can be specialized to each data point for **CQ-LVMs**.

**Lemma 5.2.** *For diagonal  $\eta_V$  in  $\mathcal{P}(\mathcal{H}_V)$ , a **DO-LVM**  $\rho(\theta)$  satisfies **Condition S** if and only if it is of the form in Theorem 5.1. The log-likelihood of these models can then expressed as  $\mathcal{L}(\theta) = \frac{1}{N} \sum_{i=1}^N \ell_i(\theta)$  where  $\ell_i(\theta) = \log P(\mathbf{v}^{(i)} | \theta)$ .*

*Proof sketch:* The proof is an application of Theorem 5.1 and is given in Appendix C.

The decomposition of the log-likelihood into terms for each datapoint, allows the training of models on real-world data since the target density operator  $\eta_V$  does not have to be initialized. We now show that **CQ-LVMs** are a broad class of models that include several Hamiltonian-based models.

**Corollary 5.3.** *A Hamiltonian-based model  $\rho(\theta) = e^{H(\theta)} / Z(\theta)$  with  $H(\theta) = \sum_r \theta_r H_r$  is a **CQ-LVMs** if and only if  $H = \oplus_i H_i$  where  $H_i$  are Hermitian operators in  $\mathcal{L}(\mathcal{H}_L)$  and  $i \in [2^{d_V}]$ .*

*Proof sketch:* The proof, due to the properties block diagonal matrices, is given in Appendix C.

We now specialize QELBO and Algorithm 1 to **CQ-LVMs**.

**Lemma 5.4.** For diagonal  $\eta_V$  in  $\mathcal{P}(\mathcal{H}_V)$  and a **CQ-LVM**  $\rho(\theta)$ , the log-likelihood of a data point  $\mathbf{v}^{(i)} \in \mathcal{D}$ ,  $\ell_i(\theta)$  is lower bounded by

$$\ell_i(\theta) \geq \text{Tr} \left( \eta_L \log(P(\mathbf{v}^{(i)}|\theta)\rho_L^{(i)}(\theta)) \right) - \text{Tr}(\sigma_L \log \sigma_L)$$

for any density operator  $\eta_L$  in  $\mathcal{P}(\mathcal{H}_L)$  with equality if and only if  $\eta_L = \rho_L^{(i)}(\theta)$ . Hence, the PRM is given by  $\mathcal{R}_\rho(\eta_V) = \oplus_i P_{\mathcal{D}}(V = v_i)\rho_L(i|\theta)$ .

*Proof sketch:* Application of Lemma 5.4 to Lemma 4.1. Proof is given in Appendix C.

This allows us to specialize Algorithm 1 to Algorithm 2, enabling the implementation of **DO-EM** without being restricted by the dimension of  $\eta_V$ . However, models such as the QBM remain intractable for real-world data due to the normalization term, a problem that exists in classical Boltzmann machines as well.

---

**Algorithm 2 DO-EM for CQ-LVM**

---

- 1: **Input:** Data and  $\theta^{(0)}$
  - 2: **while** not converged **do**
  - 3:    $\mathcal{Q}_i(\theta; \theta^{(k)}) = \text{Tr} \left( \rho_L^{(i)}(\theta^{(k)}) e^{H^{(i)}(\theta)} \right) - \log Z(\theta)$
  - 4:    $\theta^{(t+1)} = \text{argmax}_\theta \frac{1}{N} \sum_{i=1}^N \mathcal{Q}_i(\theta; \theta^{(k)})$
- 

## 5.1 Quantum Boltzmann Machine

In this section, we discuss the QBM and define variants which are amenable to implementation on high-dimensional classical data. We first describe QBMs that are **CQ-LVMs**.

**Corollary 5.5.** A  $\text{QBM}_{m,n}$  is a **CQ-LVM** if and only if quantum terms on the visible units are zero.

*Proof sketch:* The statement is true because of the structure of Pauli matrices which have entries outside the direct sum structure if and only if  $i \leq m$ . A detailed proof can be found in Appendix C.

The class of semi-quantum models studied in Demidik et al. [34] are **CQ-LVMs**. Training such a QBM is intractable for real-world data since the free energy term,  $-\log Z(\theta)$  is intractable even for classical Boltzmann machines. To achieve tractable training of QBMs, we introduce the **Quantum Interleaved Deep Boltzmann Machine (QiDBM)** that can be trained using Contrastive Divergence with a quantum Gibbs sampling step derived here.

A **Quantum Interleaved Deep Boltzmann Machine (QiDBM)** is a DBM with quantum bias terms on **non-contiguous hidden layers**. We describe the Hamiltonian of a three-layered  $\text{QiDBM}_{\ell,m,n}$  with  $\ell$  visible units and  $m$  and  $n$  hidden units respectively in the two hidden layers. For ease of presentation, the quantum bias terms are present in the middle layer.

$$H = - \sum_{i=1}^{\ell+m+n} b_i \sigma_i^z - \sum_{i=1}^{\ell} \sum_{j=1}^m w_{ij}^{(1)} \sigma_i^z \sigma_{\ell+j}^z - \sum_{i=1}^m \sum_{j=1}^n w_{ij}^{(2)} \sigma_{\ell+i}^z \sigma_{\ell+m+j}^z - \sum_{i=1}^m \Gamma_i \sigma_{\ell+i}^x \quad (\text{QiDBM})$$

The quantum interleaving in a QiDBM is necessary to make the Gibbs sampling step tractable. We illustrate the case of the middle layer of  $\text{QiDBM}_{\ell,m,n}$ . If the non-quantum visible and hidden layers are fixed to  $\mathbf{v}$  and  $\mathbf{h}^{(2)}$ , the hidden units of the quantum layer are conditionally independent. The Hamiltonian of the  $i^{\text{th}}$  unit of the quantum layer  $L^{(1)}$  is given by  $H^{L^{(1)}}(i|\mathbf{v}, \mathbf{h}^{(2)}, \theta) = -b_i^{\text{eff}} \sigma_i^z - \Gamma_i \sigma_i^x$ . This allows for the tractable sampling from the quantum layer using the expected values

$$\langle \sigma_i^z \rangle_{\mathbf{v}, \mathbf{h}^{(2)}} = \frac{b_i^{\text{eff}}}{D_i} \tanh D_i \text{ and } \langle \sigma_i^x \rangle_{\mathbf{v}, \mathbf{h}^{(2)}} = \frac{\Gamma_i}{D_i} \tanh D_i$$

where  $D_i = \sqrt{(b_i^{\text{eff}})^2 + \Gamma_i^2}$  and  $b_i^{\text{eff}} = b_i + \sum_{j=1}^{\ell} w_{ij}^{(1)} \mathbf{v}_j + \sum_{j=1}^n w_{ij}^{(2)} \mathbf{h}_j^{(2)}$ . The Gibbs step for the non-quantum layers is done as per the classical CD algorithm using the quantum sample from the  $Z$  Pauli operator. This closed-form expression for Gibbs sampling without matrices allows CD to run on a QiDBM with the same memory footprint as a DBM. See Appendix C for more details.

## 6 Empirical evaluation

In this work, we propose a quantum model **CQ-LVM**, and a general EM framework, **DO-EM**, to learn them. In this section, we empirically evaluate our methods through experiments to answer the following questions. Details of the compute used to run all our experiments and baselines are provided in Appendices D and E.

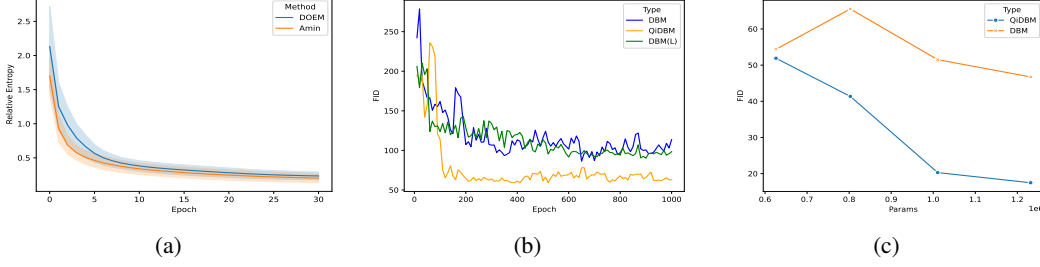


Figure 1: (a) Relative entropy during training with exact computation of a QBM on a mixture of Bernoulli distribution. Showing that DO-EM does lead to decrease in relative entropy. (b) DBM with 6272 hidden units. QiDBM with 6273 hidden units. DBM(L) with 6273 hidden units. (c) FID scores on Binarized MNIST as a function of model parameters of QiDBM and DBM.

- (Q1) **Effectiveness of DO-EM.** Is Algorithm 2, a feasible algorithm for **CQ-LVMs** compared to state of the art algorithms for QBMs ?
- (Q2) **DO-EM on Real World Data.** Does Algorithm 2 scale with the to real world data?
- (Q3) **Performance of DO-EM.** Does Algorithm 2 provide reasonable improvement in performance over classical LVMs?

To answer (Q1), we conduct experiments running exact computation to show that the proposed algorithm is feasible and is practical to implement.

**Baselines** We compare our method with our implementation of Amin et al. [12] which explores an alternate algorithm for training QBMs.

**Dataset and Metrics** We use a mixture of Bernoulli dataset introduced in Amin et al. [12] described in Appendix D. We measure the efficacy of our proposed method by measuring the average relative entropy during training.

**Results of experiment** In Figure 1a, we first observe that the relative entropy of our proposed algorithm does decrease during training, validating our theoretical results and showing, to the best of our knowledge, the first instance of an expectation maximization algorithm with quantum bias. We also observe that the performance is competitive with Amin et al. [12]. We also note that **CQ-LVM** training with DO-EM is faster than Amin et al. [12] and consumes lesser memory.

To answer (Q2) and (Q3), we conduct experiments on DBMs of varying sizes with and without the quantum bias term described in Section 5. We present qualitative results of our experiments in Appendix D.

**Baselines.** We compare our proposed method with Taniguchi et al. [22], the state of the art for training DBMs. We are unable to reproduce the results in their work and we report the results obtained from their official implementation<sup>1</sup> using the hyper parameters described in their work.

**Datasets and Metrics** Following prior work [22], we perform our experiments on MNIST and Binarized MNIST dataset [45] which contains 60,000 training images and 10,000 testing images of size 28x28. We measure the FID [46] between 10,000 generated images and the MNIST test set to assess the quality of generation. The Fréchet Inception Distance (FID) is a quantitative metric used to evaluate the quality of images generated by generative models by comparing the statistical distribution of their feature representations to those of real images.

**Experiment: Performance of DO-EM** To show the superior performance of the proposed method, we compare the FID of our proposed algorithm on Binarized MNIST. We train a QiDBM and DBM with 498, 588, 686, and 784 hidden units with a learning rate of 0.001 for 100 epochs with 2 hidden layers with SGD optimizer with a batch size of 600.

**Results of Experiments** In Figure 1c, we observe that the proposed algorithm outperforms the DBM in all cases, achieving a minimum FID of 14.77 to the DBM’s 42.61. This experiment shows that simply adding quantum bias terms to a DBM can *improve the quality* of generations by around 65%.

<sup>1</sup>[https://github.com/iShohei220/unbiased\\_dbm](https://github.com/iShohei220/unbiased_dbm)



**Experiment: DO-EM on High Dimensional Data** We run CD on 2 DBMs without quantum bias terms according to Taniguchi et al. [22] and CD with quantum bias for a QiDBM on MNIST. Each image corresponds to 6272 visible binary units. The QiDBM has 78.70M parameters with 2 hidden layers with quantum bias added to the second layer with a hidden size of 6272. Both DBMs have 2 hidden layers and have 78.69M and 78.71M parameters and hidden sizes of 6272 and 6273 respectively. We use a learning rate of 0.001 for all experiments and train with a batch size of 600 with SGD optimizer for 1000 epochs. The purpose of this experiment is to show that it is feasible to train large models with quantum bias terms.

**Results of Experiments** In Figure 1b, we observe that the proposed method outperforms both classical models of similar size with a 45% reduction in FID. We observe that the FID of the model converges to this value in around 400 epochs whereas both DBM models still exhibit instability after 500 epochs. The QiDBM achieves an FID of 62.77 whereas the classical DBMs achieve an FID of 111.73 and 99.17 for the smaller and larger model respectively. This experiment indicates that scaling QiDBMs is feasible and provides a significant improvement in performance. In Appendix D, we show the qualitative differences between generated samples of the DBM and QiDBM. We observe that the generated samples from the QiDBM appear to be better than that of the DBM after only 250 epochs.

**Discussion** We design **CQ-LVMs** and implement Algorithm 1 to learn different target distributions. We first show that Algorithm 1 is effective in learning **CQ-LVMs** and is competitive with the state of the art in terms of reduction of relative entropy at lower running times for 10 qubits and can be extended to even 20 qubits where others cannot. Next, we see that the addition of quantum bias terms to a DBM when trained using Algorithm 2 shows superior generation quality compared to classical DBMs with a 60% reduction of FID on Binarized MNIST. Next, we show that **QiDBMs** can learn high dimensional datasets like MNIST using Algorithm 2 by scaling models upto 6272 hidden units. We observe that QiDBMs also achieve better performance, with 40% lower FID compared to DBMs of similar sizes. We also observe that QiDBMs converge in about half the amount of time compared to DBMs.

## 7 Discussion

The paper makes important progress by proposing **DO-EM**, an EM Algorithm for Latent Variable models defined by Density Operators, which provably achieves likelihood ascent. We propose **CQ-LVM**, a large collection of density operator based models, where **DO-EM** applies. We show that QiDBM, an instance of **CQ-LVM**, can easily scale to MNIST dataset which requires working with 6200+ units and outperform DBMs, thus showing that Density Operator models may yield better performance. The specification of **DO-EM** is amenable to implementation on quantum devices.

**DO-EM on quantum devices** The E Step of the DO-EM algorithm can be implemented on a quantum computer using the method developed by Gilyén et al. [47], where the quantum channel is performing the partial trace operation. The goal is to prepare the Petz recovery map for the partial trace channel  $\eta^{(t)} = \mathcal{R}_\rho(\eta_V)$  using PRM. The requirements for this are (1) Quantum access to the input state  $\eta_V$  (2) efficient state preparation of the model’s density matrix  $\rho(\theta)$  [48, 49] and (3) Block-encodings for the model’s density matrix and its marginal  $\rho_V(\theta) = \text{Tr}_L \rho(\theta)$  [50]. Given these input assumptions, the quantum algorithm implementing PRM consists of three steps [47]: (1) applying  $\rho_V^{-1/2}$  on the state  $\eta_V$ , (2) applying the adjoint channel which is straight-forward for the partial trace channel and can be operationally achieved by preparing subsystem L in the maximally mixed state, and (3) applying  $\rho^{1/2}$  on the combined system. Both  $\rho_V^{-1/2}$  and  $\rho^{1/2}$  are implemented using *Quantum Singular Value Transformation (QSVT)* techniques, leveraging block-encodings of the relevant states [50].

The M Step proceeds via gradient descent by the computation of the gradient given by  $(\text{Tr}[H_r \eta(\theta^{(t)})] - \text{Tr}[H_r \rho(\theta)])$  for the different terms in the Hamiltonian  $H = \sum_r \theta_r H_r$  [14, 33]. The M Step stops when the gradients are small and an updated parameter  $\theta^{(t+1)}$  is obtained. This two-step iterative DO-EM procedure continues until convergence. While the gradients can be estimated on existing near-term quantum devices, the E step requires careful design.

## References

- [1] J. Preskill. Quantum computing in the nisq era and beyond. *Quantum*, 2:79, 2018.
- [2] Michael A. Nielsen and Isaac L. Chuang. *Quantum Computation and Quantum Information: 10th Anniversary Edition*. Cambridge University Press, 2010. doi: 10.1017/CBO9780511976667.
- [3] Yaswitha Gujju, Atsushi Matsuo, and Rudy Raymond. Quantum machine learning on near-term quantum devices: Current state of supervised and unsupervised techniques for real-world applications. *Phys. Rev. Appl.*, 21:067001, Jun 2024.
- [4] Christopher M. Bishop. *Pattern Recognition and Machine Learning*. Springer, New York, 2006. ISBN 978-0-387-31073-2.
- [5] Michael I. Jordan, Zoubin Ghahramani, Tommi S. Jaakkola, and Lawrence K. Saul. An introduction to variational methods for graphical models. *Machine Learning*, 37(2):183–233, 1999. doi: 10.1023/A:1007665907178.
- [6] Zoubin Ghahramani. An introduction to hidden markov models and bayesian networks. *International Journal of Pattern Recognition and Artificial Intelligence*, 15(01):9–42, 2001.
- [7] Diederik P Kingma and Max Welling. Auto-encoding variational bayes. *arXiv preprint arXiv:1312.6114*, 2014.
- [8] Ian Goodfellow, Jean Pouget-Abadie, Mehdi Mirza, Bing Xu, David Warde-Farley, Sherjil Ozair, Aaron Courville, and Yoshua Bengio. Generative adversarial nets. In *Advances in neural information processing systems*, volume 27, 2014.
- [9] Jonathan Ho, Ajay Jain, and Pieter Abbeel. Denoising diffusion probabilistic models. In *Advances in Neural Information Processing Systems*, volume 33, pages 6840–6851, 2020.
- [10] Leonard E. Baum and Ted Petrie. Statistical Inference for Probabilistic Functions of Finite State Markov Chains. *The Annals of Mathematical Statistics*, 37(6):1554 – 1563, 1966.
- [11] A. P. Dempster, N. M. Laird, and D. B. Rubin. Maximum likelihood from incomplete data via the em algorithm. *Journal of the Royal Statistical Society: Series B (Methodological)*, 39(1): 1–22, 1977.
- [12] Mohammad H. Amin, Evgeny Andriyash, Jason Rolfe, Bohdan Kulchytskyy, and Roger Melko. Quantum boltzmann machine. *Phys. Rev. X*, 8:021050, May 2018.
- [13] Mária Kieferová and Nathan Wiebe. Tomography and generative training with quantum boltzmann machines. *Phys. Rev. A*, 96:062327, 12 2017.
- [14] H J Kappen. Learning quantum models from quantum or classical data. *Journal of Physics A: Mathematical and Theoretical*, 53(21):214001, 5 2020.
- [15] Rajendra Bhatia. *Matrix Analysis*, volume 169. Springer, 1997. ISBN 0387948465.
- [16] David H. Ackley, Geoffrey E. Hinton, and Terrence J. Sejnowski. A learning algorithm for boltzmann machines. *Cognitive Science*, 9(1):147–169, 1985. ISSN 0364-0213.
- [17] P. Smolensky. Information processing in dynamical systems: Foundations of harmony theory. In *Parallel Distributed Processing, Volume 1: Explorations in the Microstructure of Cognition: Foundations*, chapter 6, pages 194–281. The MIT Press, 07 1986.
- [18] Geoffrey E Hinton. Training products of experts by minimizing contrastive divergence. *Neural Comput*, 14(8):1771–1800, Aug 2002.
- [19] Miguel Á. Carreira-Perpiñán and Geoffrey Hinton. On contrastive divergence learning. In Robert G. Cowell and Zoubin Ghahramani, editors, *Proceedings of the Tenth International Workshop on Artificial Intelligence and Statistics*, volume R5 of *Proceedings of Machine Learning Research*, pages 33–40. PMLR, 06–08 Jan 2005.

- [20] Ruslan Salakhutdinov and Geoffrey Hinton. Deep boltzmann machines. In *Proceedings of the 12th International Conference on Artificial Intelligence and Statistics (AISTATS)*, volume 5 of *JMLR: W&CP*, pages 448–455, Clearwater Beach, Florida, USA, 2009. JMLR.
- [21] Ruslan Salakhutdinov and Geoffrey E. Hinton. An efficient learning procedure for deep boltzmann machines. *Neural Computation*, 24(8):1967–2006, 2012. doi: 10.1162/NECO\_a\_00302.
- [22] Shohei Taniguchi, Masahiro Suzuki, Yusuke Iwasawa, and Yutaka Matsuo. End-to-end training of deep boltzmann machines by unbiased contrastive divergence with local mode initialization. In Andreas Krause, Emma Brunskill, Kyunghyun Cho, Barbara Engelhardt, Sivan Sabato, and Jonathan Scarlett, editors, *Proceedings of the 40th International Conference on Machine Learning*, volume 202 of *Proceedings of Machine Learning Research*, pages 33804–33815. PMLR, 23–29 Jul 2023.
- [23] Mark M. Wilde. *Quantum Information Theory*. Cambridge University Press, nov 2016.
- [24] H. Umegaki. Conditional expectation in an operator algebra. IV (entropy and information). *Kōdai Mathematical Seminar Reports*, 14:59–85, 1962.
- [25] Göran Lindblad. Completely positive maps and entropy inequalities. *Communications in Mathematical Physics*, 40(2):147–151, Jun 1975.
- [26] Dénes Petz. Sufficient subalgebras and the relative entropy of states of a von neumann algebra. *Communications in Mathematical Physics*, 105(1):123–131, Mar 1986.
- [27] Dénes Petz. Sufficiency Of Channels Over von Neumann Algebras. *The Quarterly Journal of Mathematics*, 39(1):97–108, 03 1988.
- [28] Mary Beth Ruskai. Inequalities for quantum entropy: A review with conditions for equality. *Journal of Mathematical Physics*, 43(9):4358–4375, sep 2002.
- [29] N. J. Cerf and C. Adami. Negative entropy and information in quantum mechanics. *Phys. Rev. Lett.*, 79:5194–5197, Dec 1997.
- [30] Nathan Wiebe and Leonard Wossnig. Generative training of quantum boltzmann machines with hidden units. *arXiv preprint arXiv:1905.09902*, 2019.
- [31] Onno Huijgen, Luuk Coopmans, Peyman Najafi, Marcello Benedetti, and Hilbert J. Kappen. Training quantum boltzmann machines with the  $\beta$ -variational quantum eigensolver. *arXiv preprint arXiv:2304.08631*, 2024.
- [32] Dhruvil Patel and Mark M. Wilde. Natural gradient and parameter estimation for quantum boltzmann machines. *arXiv preprint arXiv:2410.24058*, 2024.
- [33] Luuk Coopmans and Marcello Benedetti. On the sample complexity of quantum boltzmann machine learning. *Communications Physics*, 7(1):274, 2024.
- [34] Maria Demidik, Cenk Tüysüz, Nico Piatkowski, Michele Grossi, and Karl Jansen. Expressive equivalence of classical and quantum restricted boltzmann machines. *arXiv preprint arXiv:2502.17562*, 2025.
- [35] Manfred K. Warmuth and Dima Kuzmin. Bayesian generalized probability calculus for density matrices. *Mach. Learn.*, 78(1–2):63–101, January 2010.
- [36] Thomas M. Cover and Joy A. Thomas. *Elements of Information Theory*. Wiley-Interscience, USA, 2006.
- [37] David R. Hunter Kenneth Lange and Ilsoon Yang. Optimization transfer using surrogate objective functions. *Journal of Computational and Graphical Statistics*, 9(1):1–20, 2000. doi: 10.1080/10618600.2000.10474858.
- [38] Jan de Leeuw. Block-relaxation algorithms in statistics. In Hans-Hermann Bock, Wolfgang Lenski, and Michael M. Richter, editors, *Information Systems and Data Analysis*, pages 308–324, Berlin, Heidelberg, 1994. Springer Berlin Heidelberg. ISBN 978-3-642-46808-7.

- [39] Andrew Lesniewski and Mary Beth Ruskai. Monotone riemannian metrics and relative entropy on noncommutative probability spaces. *Journal of Mathematical Physics*, 40(11):5702–5724, 11 1999.
- [40] Mario Berta, Marius Lemm, and Mark M. Wilde. Monotonicity of quantum relative entropy and recoverability. *Quantum Info. Comput.*, 15(15–16):1333–1354, November 2015.
- [41] Mark M. Wilde. Recoverability in quantum information theory. *Proceedings of the Royal Society A: Mathematical, Physical and Engineering Sciences*, 471(2182):20150338, oct 2015.
- [42] Eric A Carlen and Anna Vershynina. Recovery map stability for the data processing inequality. *Journal of Physics A: Mathematical and Theoretical*, 53(3):035204, jan 2020.
- [43] Samuel S. Cree and Jonathan Sorce. Geometric conditions for saturating the data processing inequality. *Journal of Physics A: Mathematical and Theoretical*, 55(13):135301, 2022. doi: 10.1088/1751-8121/ac5648.
- [44] Hideitsu Hino, Shotaro Akaho, and Noboru Murata. Geometry of em and related iterative algorithms. *Information Geometry*, 7(1):39–77, 2024.
- [45] Li Deng. The mnist database of handwritten digit images for machine learning research [best of the web]. *IEEE Signal Processing Magazine*, 29(6):141–142, 2012.
- [46] Maximilian Seitzer. pytorch-fid: FID Score for PyTorch. <https://github.com/mseitzer/pytorch-fid>, August 2020. Version 0.3.0.
- [47] András Gilyén, Seth Lloyd, Iman Marvian, Yihui Quek, and Mark M. Wilde. Quantum algorithm for petz recovery channels and pretty good measurements. *Phys. Rev. Lett.*, 128:220502, Jun 2022.
- [48] Ersen Bilgin and Sergio Boixo. Preparing thermal states of quantum systems by dimension reduction. *Phys. Rev. Lett.*, 105:170405, Oct 2010. doi: 10.1103/PhysRevLett.105.170405.
- [49] Chi-Fang Chen, Michael J. Kastoryano, Fernando G. S. L. Brandão, and András Gilyén. Quantum thermal state preparation, 2023.
- [50] András Gilyén, Yuan Su, Guang Hao Low, and Nathan Wiebe. Quantum singular value transformation and beyond: exponential improvements for quantum matrix arithmetics. In *Proceedings of the 51st Annual ACM SIGACT Symposium on Theory of Computing*, STOC 2019, page 193–204, New York, NY, USA, 2019. Association for Computing Machinery. ISBN 9781450367059. doi: 10.1145/3313276.3316366.
- [51] Yixuan Qiu, Lingsong Zhang, and Xiao Wang. Unbiased contrastive divergence algorithm for training energy-based latent variable models. In *International Conference on Learning Representations*, 2020.
- [52] Iordanis Kerenidis, Jonas Landman, Alessandro Luongo, and Anupam Prakash. q-means: A quantum algorithm for unsupervised machine learning. In H. Wallach, H. Larochelle, A. Beygelzimer, F. d’Alché Buc, E. Fox, and R. Garnett, editors, *Advances in Neural Information Processing Systems 32*, pages 4136–4146. Curran Associates, Inc., 2019.
- [53] Iordanis Kerenidis, Alessandro Luongo, and Anupam Prakash. Quantum expectation-maximization for Gaussian mixture models. In Hal Daumé III and Aarti Singh, editors, *Proceedings of the 37th International Conference on Machine Learning*, volume 119 of *Proceedings of Machine Learning Research*, pages 5187–5197. PMLR, 7 2020.
- [54] Hideyuki Miyahara, Kazuyuki Aihara, and Wolfgang Lechner. Quantum expectation-maximization algorithm. *Phys. Rev. A*, 101(1):012326, 2020. doi: 10.1103/PhysRevA.101.012326.
- [55] Youngseok Kim, Andrew Eddins, Sajant Anand, Ken Xuan Wei, Ewout van den Berg, Sami Rosenblatt, Hasan Nayfeh, Yantao Wu, Michael Zaletel, Kristan Temme, and Abhinav Kandala. Evidence for the utility of quantum computing before fault tolerance. *Nature*, 618(7965): 500–505, Jun 2023. ISSN 1476-4687. doi: 10.1038/s41586-023-06096-3.

- [56] Jacob Biamonte, Peter Wittek, Nicola Pancotti, Patrick Rebentrost, Nathan Wiebe, and Seth Lloyd. Quantum machine learning. *Nature*, 549(7671):195–202, 9 2017.
- [57] M. Schuld, I. Sinayskiy, and F. Petruccione. An introduction to quantum machine learning. *Contemporary Physics*, 56(2):172–185, 2015.
- [58] Patrick Hayden, Richard Jozsa, Dénes Petz, and Andreas Winter. Structure of states which satisfy strong subadditivity of quantum entropy with equality. *Communications in Mathematical Physics*, 246(2):359–374, 2004. doi: 10.1007/s00220-004-1049-z.
- [59] Dhruvil Patel, Daniel Koch, Saahil Patel, and Mark M. Wilde. Quantum boltzmann machine learning of ground-state energies. *arXiv preprint arXiv:2410.12935*, 2024.
- [60] Eric R. Anschuetz and Yudong Cao. Realizing quantum boltzmann machines through eigenstate thermalization. *arXiv preprint arXiv:1903.01359*, 2019.
- [61] Christa Zoufal, Aurélien Lucchi, and Stefan Woerner. Variational quantum boltzmann machines. *Quantum Machine Intelligence*, 3(1):7, 2021.
- [62] Zhiyan Ding, Bowen Li, and Lin Lin. Efficient quantum gibbs samplers with kubo–martin–schwinger detailed balance condition. *Communications in Mathematical Physics*, 406(3):67, Feb 2025. ISSN 1432-0916. doi: 10.1007/s00220-025-05235-3.
- [63] Marcello Benedetti, John Realpe-Gómez, Rupak Biswas, and Alejandro Perdomo-Ortiz. Quantum-assisted learning of hardware-embedded probabilistic graphical models. *Phys. Rev. X*, 7:041052, Nov 2017. doi: 10.1103/PhysRevX.7.041052.
- [64] Jon Nelson, Marc Vuffray, Andrey Y. Lokhov, Tameem Albash, and Carleton Coffrin. High-quality thermal gibbs sampling with quantum annealing hardware. *Phys. Rev. Appl.*, 17:044046, Apr 2022. doi: 10.1103/PhysRevApplied.17.044046.
- [65] Ryosuke Shibukawa, Ryo Tamura, and Koji Tsuda. Boltzmann sampling with quantum annealers via fast stein correction. *Phys. Rev. Res.*, 6:043050, Oct 2024. doi: 10.1103/PhysRevResearch.6.043050.

## Appendix

In this appendix, we provide the following material.

- In Appendix A, we discuss Boltzmann machines and the Contrastive Divergence algorithm.
- In Appendix B, we provided a discussion on density operators, quantum channels, and related work in training density operator models.
- In Appendix C, we provide the proofs of the theoretical results proposed in the main body.
- In Appendix D, we provide implementation details and additional experiments with the **DO-EM** algorithm.
- In Appendix E, we discuss the computational setup used in our experiments.
- In Appendix F, we discuss the limitations of this work.

### A Boltzmann machines

The *Contrastive Divergence* (CD) [18, 19] algorithm samples the hidden state for a data point through an iterative sampling scheme to efficiently compute the parameters to model a target distribution by approximating the gradient of the log-likelihood. Building on recent advances in the contrastive divergence method [51], DBMs trained using CD was studied in Taniguchi et al. [22]. We describe the CD Algorithm for a Restricted Boltzmann Machine (RBM), a special case of a DBM with a single layer. Formally, an  $\text{RBM}_{m,n}$  is a single layer DBM consisting of a visible layer  $\mathbf{v} \in \{0, 1\}^m$  and a hidden layer  $\mathbf{h} \in \{0, 1\}^n$ , parameterized by weight matrix  $\mathbf{W} \in \mathbb{R}^{m \times n}$ , bias vectors  $\mathbf{a} \in \mathbb{R}^m$  (visible) and  $\mathbf{b} \in \mathbb{R}^n$  (hidden). The energy function is given by  $E(\mathbf{v}, \mathbf{h}) = -\mathbf{v}^\top \mathbf{W} \mathbf{h} - \mathbf{a}^\top \mathbf{v} - \mathbf{b}^\top \mathbf{h}$ . At the  $t^{\text{th}}$  time step with parameters  $\mathbf{W}^{(t)}, \mathbf{a}^{(t)}, \mathbf{b}^{(t)}$ ,  $K$  iterations of sampling is used to sample visible and hidden units. Formally,

$$\begin{aligned} h_j^{(k)} &\sim P(h_j = 1 \mid \mathbf{v}^{(k)}) = \sigma \left( \sum_i W_{ij}^{(t)} v_i^{(k)} + b_j^{(t)} \right) \\ v_i^{(k+1)} &\sim P(v_i = 1 \mid \mathbf{h}^{(k)}) = \sigma \left( \sum_j W_{ij}^{(t)} h_j^{(k)} + a_i^{(t)} \right) \end{aligned}$$

where  $\sigma(x) = \frac{1}{1+e^{-x}}$  is the sigmoid function and  $\mathbf{v}^{(0)} = \mathbf{v}$  and  $k \in [K]$ . The parameter updates at the  $t^{\text{th}}$  step, with learning rate  $\gamma$  is then,

$$\begin{aligned} W_{ij}^{(t+1)} &= W_{ij}^{(t)} + \gamma \left( v_i h_j^{(0)} - v_i^{(K)} h_j^{(K)} \right) \\ a_i^{(t+1)} &= a_i^{(t)} + \gamma \left( v_i - v_i^{(K)} \right) \\ b_j^{(t+1)} &= b_j^{(t)} + \gamma \left( h_j^{(0)} - h_j^{(K)} \right). \end{aligned}$$

### B Density operators

Current research explores leveraging quantum mechanics for machine learning either by achieving computational speedups with quantum hardware [52–55], or by capturing more complex data structures through quantum formalisms [56, 57]. The use of density operators, quantum generalizations of classical probability distributions, to model data represents an effort in the latter direction.

A density operator on a Hilbert space  $\mathcal{H}$  is a Hermitian, positive semi-definite operator with unit trace [2, 23]. The set of Density operators will be denoted by  $\mathcal{P}(\mathcal{H})$ , and can be regarded as generalizations of probability distributions. We now define quantum channels that act on density operators.

Let  $\mathcal{S}(\mathcal{H})$  denote the set of square linear operators on a finite dimensional Hilbert space  $\mathcal{H}$ . A linear map  $\mathcal{N} : \mathcal{S}(\mathcal{H}_A) \rightarrow \mathcal{S}(\mathcal{H}_B)$  is *positive* if  $\mathcal{N}(X)$  is positive semi-definite for all positive semi-definite operators  $X$  in  $\mathcal{S}(\mathcal{H})$ . Such a map is *completely positive* if  $\mathbf{I}_R \otimes \mathcal{N}$  is a positive map for an arbitrary reference system  $R$ . A map is *trace preserving* if  $\text{Tr}(\mathcal{N}(X)) = \text{Tr}(X)$ .

**Definition B.1** (Quantum Channel). A quantum channel  $\mathcal{N} : \mathcal{S}(\mathcal{H}_A) \rightarrow (\mathcal{H}_B)$  is a linear, completely positive, trace preserving map.

We now define an inner product on operators.

**Definition B.2** (Hilbert-Schmidt Inner Product). The Hilbert-Schmidt Inner Product between two operators  $X, Y$  in  $\mathcal{S}(\mathcal{H})$  is defined as  $\langle X, Y \rangle = \text{Tr}(X^\dagger Y)$ .

The inner product allows us to define the adjoint of a quantum channel.

**Definition B.3.** The *adjoint* of a quantum channel  $\mathcal{N} : \mathcal{S}(\mathcal{H}_A) \rightarrow (\mathcal{H}_B)$  is the unique linear map  $\mathcal{N}^\dagger : \mathcal{S}(\mathcal{H}_B) \rightarrow (\mathcal{H}_A)$  satisfying  $\langle Y, \mathcal{N}(X) \rangle = \langle \mathcal{N}^\dagger(Y), X \rangle$  for all  $X$  in  $\mathcal{S}(\mathcal{H}_A)$  and  $Y$  in  $\mathcal{S}(\mathcal{H}_B)$ .

Lindblad [25] showed that the relative entropy is monotonic under the action of a quantum channel.

**Theorem B.4** (Monotonicity of Relative Entropy). *For density operators  $\omega$  and  $\rho$  in  $\mathcal{P}(\mathcal{H}_A \otimes \mathcal{H}_B)$  such that  $\ker(\omega) \subset \ker(\rho)$ ,  $D_U(\omega, \rho) \geq D_U(\mathcal{N}(\omega), \mathcal{N}(\rho))$ .*

Petz [26, 27] showed that MRE is saturated if and only if the Petz Recovery Map reverses the quantum channel. We provide a restatement of this result from Hayden et al. [58].

**Theorem B.5.** *For states  $\omega$  and  $\rho$ ,  $D_U(\omega, \rho) = D_U(\mathcal{N}(\omega), \mathcal{N}(\rho))$  if and only if there exists a quantum channel  $\mathcal{R}$  such that  $\mathcal{R}(\mathcal{N}(\omega)) = \omega$  and  $\mathcal{R}(\mathcal{N}(\rho)) = \rho$ . Furthermore, on the support of  $\mathcal{N}(\rho)$ ,  $\mathcal{R}$  can be given explicitly by the formula*

$$\mathcal{R}(\alpha) = \rho^{1/2} \mathcal{N}^\dagger \left( \mathcal{N}(\rho)^{-1/2} \alpha \mathcal{N}(\rho)^{-1/2} \right) \rho^{1/2}.$$

This lead to the definition of the Petz Recovery Map.

**Definition B.6** (Petz Recovery Map). For a density operator  $\rho$  in  $\mathcal{P}(\mathcal{H}_A)$ , the Petz Recovery Map for a quantum channel  $\mathcal{N} : \mathcal{S}(\mathcal{H}_A) \rightarrow \mathcal{S}(\mathcal{H}_B)$  is the map  $\mathcal{R}_{\mathcal{N}, \rho} : \mathcal{H}_B \rightarrow \mathcal{H}_A$  defined by

$$\mathcal{R}_{\mathcal{N}, \rho}(\alpha) = \rho^{1/2} \mathcal{N}^\dagger \left( \mathcal{N}(\rho)^{-1/2} \alpha \mathcal{N}(\rho)^{-1/2} \right) \rho^{1/2}.$$

The Petz Recovery Map is a completely positive, trace non-increasing map [23] that does not always map density operators to density operators. Ruskai [28] proved an equivalent condition for the saturation of MRE.

**Theorem B.7** (Ruskai's condition). *For density operators  $\omega$  and  $\rho$  in  $\mathcal{P}(\mathcal{H}_A \otimes \mathcal{H}_B)$  such that  $\ker(\omega) \subset \ker(\rho)$ ,  $D_U(\mathcal{N}(\omega), \mathcal{N}(\rho)) = D_U(\omega, \rho)$  if and only if  $\log \omega - \log \rho = \mathcal{N}^\dagger(\mathcal{N}(\omega) - \mathcal{N}(\rho))$ .*

In this work, we focus on the quantum channel defined by the partial trace operation  $\mathcal{N}(\rho) = \text{Tr}_B \rho$  and its adjoint  $\mathcal{N}^\dagger(\rho_A) = \rho_A \otimes \mathbb{I}_B$ . All our results are specialized to this case.

## B.1 Related work on Density Operator Models

Most recent works on density operator models (**DOMs**) consider settings without hidden units [14, 32, 59, 31] due to operator-theoretic difficulties brought about by the partial trace operation during gradient evaluation [30]. Other studies considered hidden variable **DOMs**, where the gradient evaluation was accomplished using heuristic methods [12, 60, 61]. As such, these methods rely on the approximate (variational) preparation of the quantum Gibbs state density matrix [48, 49, 62]. Sampling from a Gibbs state distribution can also be performed using a quantum annealer, which may offer advantages even for classical machine learning models [12, 63–65].

These existing approaches rarely scale beyond 12 visible units—limited by restricted access to quantum hardware, the exponential cost of simulating quantum systems, and the memory bottlenecks associated with representing and optimizing **DO-LVMs** on classical devices. EM based algorithms can provide a simpler alternative to existing learning algorithms for **DO-LVMs** which directly maximizes the likelihood. However deriving such algorithms in the density operator theoretic setup is extremely challenging for a variety of reasons. *Most notably operator theoretic analogues of classical inequalities, such as the Jensen Inequality, cannot be directly applied to derive an Evidence lower bound (ELBO) for DO-LVMs.*

## C Proofs

### Proof of Lemma 4.1

**Lemma (Quantum ELBO).** *Let  $\mathcal{J}(\eta_v) = \{\eta \mid \eta \in \mathcal{P}(\mathcal{H}_V \otimes \mathcal{H}_L) \text{ \& } \text{Tr}_L \eta = \eta_v\}$  be the set of feasible extensions for a target  $\eta_v \in \mathcal{P}(\mathcal{H}_V)$ . Then for a **DO-LVM**  $\rho(\theta)$  and  $\eta \in \mathcal{J}(\eta_v)$ ,*

$$\mathcal{L}(\theta) \geq \text{QELBO}(\eta, \theta) = \text{Tr}(\eta \log \rho(\theta)) + S(\eta) - S(\eta_v).$$

*Proof.* Since  $\eta \in \mathcal{J}(\eta_v)$ ,  $\text{Tr}_L(\eta) = \eta_v$  and  $\text{Tr}_L \rho(\theta) = \rho_v(\theta)$ . From MRE,

$$\begin{aligned} D_U(\eta, \rho(\theta)) &\geq D_U(\eta_v, \rho_v(\theta)), \\ \text{Tr}(\eta \log \eta) - \text{Tr}(\eta \log \rho(\theta)) &\geq \text{Tr}(\eta_v \log \eta_v) - \text{Tr}(\eta_v \log \rho_v(\theta)), \\ \text{Tr}(\eta_v \log \rho_v(\theta)) &\geq \text{Tr}(\eta \log \rho(\theta)) - \text{Tr}(\eta \log \eta) + \text{Tr}(\eta_v \log \eta_v), \\ \mathcal{L}(\theta) &\geq \text{Tr}(\eta \log \rho(\theta)) + S(\eta) - S(\eta_v). \end{aligned}$$

□

This proof reduces to a proof of the classical ELBO from the chain rule of KL divergence [36] when  $\rho(\theta)$  is diagonal.

### Proof of Theorem 4.3

We first prove a useful lemma.

**Lemma C.1.** *The Petz recovery map with respect to a quantum channel  $\mathcal{N}$  and density operator  $\rho$  is trace preserving if  $\rho$  is full rank.*

*Proof.* This statement is a consequence of the cyclic property of trace and the definition of the adjoint CPTP map  $\mathcal{N}^\dagger$ .

$$\begin{aligned} \text{Tr}(\mathcal{P}_{\rho, \mathcal{N}}(\omega)) &= \text{Tr}(\rho^{1/2} \mathcal{N}^\dagger(\mathcal{N}(\rho)^{-1/2} \omega \mathcal{N}(\rho)^{-1/2}) \rho^{1/2}) \\ &= \text{Tr}(\rho \mathcal{N}^\dagger(\mathcal{N}(\rho)^{-1/2} \omega \mathcal{N}(\rho)^{-1/2})) \\ &= \text{Tr}(\mathcal{N}(\rho) \mathcal{N}(\rho)^{-1/2} \omega \mathcal{N}(\rho)^{-1/2}) \\ &= \text{Tr}(\mathcal{N}(\rho)^{1/2} \mathcal{N}(\rho)^{-1/2} \omega \mathcal{N}(\rho)^{-1/2} \mathcal{N}(\rho)^{1/2}) \\ &= \text{Tr}(\mathbf{I} \omega \mathbf{I}) \\ &= \text{Tr}(\omega). \end{aligned}$$

□

This theorem requires  $\rho$  to be full rank for  $\text{Tr}(\mathcal{N}(\rho)^{1/2} \mathcal{N}(\rho)^{-1/2}) = \mathbf{I}$  since CPTP maps full rank matrices to full rank matrices. We now restate **Condition S** and Theorem 4.3.

**Definition 1 (Condition S).** Two density operators  $\omega$  in  $\mathcal{P}(\mathcal{H}_A)$  and  $\rho$  in  $\mathcal{P}(\mathcal{H}_A \otimes \mathcal{H}_B)$  satisfy the sufficiency condition if  $\rho$  is full rank, separable, and  $[\omega, \text{Tr}_B(\rho)] = 0$  such that

$$\rho = \sum_{i=1}^{d_A} \alpha_i \mathbf{x}_i \mathbf{x}_i^\dagger \otimes \rho_B^{(i)}$$

where  $\{\mathbf{x}_i\}_{i=1}^{d_A}$  is an orthonormal basis of  $\mathcal{H}_A$  and  $\rho_B^{(i)} \in \mathcal{P}(\mathcal{H}_B)$ .

**Theorem.** *Suppose two density operators  $\omega$  in  $\mathcal{P}(\mathcal{H}_A)$  and  $\rho$  in  $\mathcal{P}(\mathcal{H}_A \otimes \mathcal{H}_B)$  such that **Condition S** is satisfied, the solution to the information projection problem QIP is PRM.*

*Proof.* Since  $\rho$  is full rank, the Petz recovery map gives a valid density operator by Lemma C.1. Moreover, **Condition S** guarantees that  $[\rho, \rho_A \otimes \mathbf{I}_B] = 0$  and that  $\text{Tr}_B \mathcal{R}_{\rho, \text{Tr}_L}(\omega) = \omega$ .

As mentioned in the main body of the paper, we prove this theorem by showing that the Petz recovery map commutes with  $\rho$ . Since  $[\omega, \text{Tr}_B(\rho)] = 0$  and  $[\rho, \text{Tr}_B(\rho) \otimes \mathbf{I}_B] = 0$ , we know that



$[\rho, \omega \otimes \mathbf{I}_B] = 0$ . Note that if two matrices commute, their squareroots also commute because they share the same eigenspace. Since the Petz recovery map with respect to  $\rho$  and  $\text{Tr}_B$  is equal to

$$\mathcal{P}_{\rho, \text{Tr}_B}(\tilde{\sigma}) = \rho^{1/2}((\text{Tr}_B(\rho)^{-1/2} \omega \text{Tr}_B(\rho)^{-1/2}) \otimes \mathbf{I}_B) \rho^{1/2},$$

we know that  $[\mathcal{P}_{\rho, \text{Tr}_B}(\omega), \rho] = 0$ .

We now show that the Petz recovery map and  $\rho$  satisfy the Ruskai condition.

$$\begin{aligned} \log \rho - \log \mathcal{R}_{\rho, \text{Tr}_B}(\omega) &= \log \rho - \log(\rho^{1/2}((\text{Tr}_B(\rho)^{-1/2} \omega \text{Tr}_B(\rho)^{-1/2}) \otimes \mathbf{I}_B) \rho^{1/2}) \\ &= \log \rho - \log(\rho((\text{Tr}_B(\rho)^{-1} \omega) \otimes \mathbf{I}_B)) \\ &= \log \rho - \log \rho - \log(\text{Tr}_B(\rho)^{-1} \omega \otimes \mathbf{I}_B) \\ &= \log(\text{Tr}_B(\rho) \otimes \mathbf{I}_B) - \log(\omega \otimes \mathbf{I}_B) \\ &= (\log(\text{Tr}_B(\rho)) - \log(\omega)) \otimes \mathbf{I}_B. \end{aligned}$$

Hence, PRM attains the minimum possible value in the QIP problem and is the information projection of  $\rho$  on to the set of density operators that partial trace to  $\omega$ .  $\square$

#### Proof of Theorem 4.4

**Theorem** ( $\mathcal{Q}$  is a minorant). *Let  $\eta_v$  be a target density matrix and  $\rho(\theta)$  be a **DO-LVM** trained by the **DO-EM** algorithm. If  $\rho(\theta^{(t)})$  and its QIP onto the set of feasible extensions,  $\eta^{(t)}$ , obey Ruskai's condition, then  $\mathcal{Q}$  is a minorant of the log-likelihood. Then,  $\mathcal{L}(\theta^{(t+1)}) \geq \mathcal{L}(\theta^{(t)})$ , where  $\theta^{(t+1)} = \arg\max_{\theta} \mathcal{Q}(\theta; \theta^{(t)})$ .*

*Proof.* From the Ruskai condition, we obtain

$$\mathcal{L}(\theta^{(t)}) = \mathcal{Q}(\theta^{(t)}, \theta^{(t)}). \quad (1)$$

By the definition of  $\theta^{(t+1)}$ ,

$$\mathcal{Q}(\theta^{(t)}, \theta^{(t)}) \leq \mathcal{Q}(\theta^{(t)}, \theta^{(t+1)}). \quad (2)$$

Combining these inequalities with the QELBO, we obtain

$$\begin{aligned} \mathcal{L}(\theta^{(t+1)}) &\geq \mathcal{Q}(\theta^{(t)}, \theta^{(t+1)}); \\ \mathcal{L}(\theta^{(t+1)}) &\geq \mathcal{Q}(\theta^{(t)}, \theta^{(t)}) \quad \text{by (2);} \\ \mathcal{L}(\theta^{(t+1)}) &\geq \mathcal{L}(\theta^{(t)}) \quad \text{by (1).} \end{aligned}$$

$\square$

#### Proof of Corollary 4.5

**Corollary.** *For a target density operator  $\eta_v$  and model  $\rho(\theta)$  satisfying **Condition S**, the E step is the Petz recovery map  $\mathcal{R}_{\rho}(\eta_v)$ . Moreover, such a model trained using the **DO-EM** algorithm achieves provable likelihood ascent at every iteration.*

*Proof.* We proved in Theorem 4.3 that the Petz Recovery Map satisfies the Ruskai condition under **Condition S**. Hence, the statement is an immediate corollary to Theorem 4.4.  $\square$

#### Proof of Corollary 4.6

**Corollary.** *For a Hamiltonian-based model with E step solution  $\eta^{(t)}$ , the M step reduces to*

$$\theta^{(t+1)} = \arg\max_{\theta} \text{Tr}(\eta^{(t)} \mathbf{H}(\theta)) - \log Z(\theta)$$

*Proof.* Let  $\rho(\theta) = \frac{1}{Z(\theta)} e^{\mathbf{H}(\theta)}$  be a Hamiltonian-based model. For a Hermitian matrix  $A$  that is diagonalized as  $A = U \Lambda U^\dagger$ , the matrix logarithm can be expressed as  $\log A = U \log(\Lambda) U^\dagger$ .

Applying this to  $\rho(\theta)$ , we obtain

$$\begin{aligned}\log(\rho(\theta)) &= U \log\left(\frac{1}{Z(\theta)}\Lambda\right) U^\dagger \\ &= U \log(\Lambda) U^\dagger - \log(Z(\theta))\mathbf{I} \\ &= \mathbf{H}(\theta) - \log(Z(\theta))\mathbf{I}.\end{aligned}$$

The result follows since  $\text{Tr}(\eta^{(t)} \log(Z(\theta))\mathbf{I}) = \log(Z(\theta))\text{Tr}(\eta^{(t)}\mathbf{I}) = \log(Z(\theta))$ .  $\square$

### Proof of Theorem 5.1

**Theorem.** If  $\rho_V$  is diagonal,  $\rho$  satisfies **Condition S** if and only if  $\rho = \oplus_i \rho_L(i)$  and  $P(\mathbf{v}_i) = \text{Tr}(\rho_L(i))$  with  $\mathbf{v}_i \in \mathfrak{B}$ . The density operator for  $\mathcal{H}_L$  for a particular  $\mathbf{v}_i$  is then given by  $\frac{1}{P(\mathbf{v}_i)}\rho_L(i)$ .

*Proof.* Since  $\rho$  satisfies **Condition S**, we know that

$$\rho = \sum_{i=1}^{d_V} \alpha_i \mathbf{x}_i \mathbf{x}_i^\dagger \otimes \rho_L^{(i)}$$

where  $\{\mathbf{x}_i\}_{i=1}^{d_V}$  is an orthonormal basis of  $\mathcal{H}_V$  and  $\rho_L^{(i)} \in \mathcal{P}(\mathcal{H}_L)$ . Since  $\rho_V$  is diagonal and  $\rho_V = \sum_{i=1}^{d_V} \alpha_i \mathbf{x}_i \mathbf{x}_i^\dagger$ , we conclude that  $\{\mathbf{x}_i\}$  is the standard basis of  $\mathcal{H}_V$ ; each  $\mathbf{x}_i$  has a 1 at the  $i^{\text{th}}$  position and zeros elsewhere. Hence,  $\rho = \oplus_i \rho_L(i)$ . The matrices  $\frac{1}{\text{Tr}(\rho_L(i))}\rho_L(i)$  are valid conditional density operators since projecting the matrix  $\rho$  onto  $\mathbf{x}_i \mathbf{x}_i^\dagger \otimes \mathbf{I}_L$  zeroes out all other components.  $\square$

### Proof of Lemma 5.2

**Lemma.** For diagonal  $\eta_V$  in  $\mathcal{P}(\mathcal{H}_V)$ , a **DO-LVM**  $\rho(\theta)$  satisfies **Condition S** if and only if it is of the form in Theorem 5.1. The log-likelihood of these models can then be expressed as  $\mathcal{L}(\theta) = \frac{1}{N} \sum_{i=1}^N \ell_i(\theta)$  where  $\ell_i(\theta) = \log P(\mathbf{v}^{(i)} | \theta)$ .

*Proof.* The log-likelihood is given by  $\mathcal{L}(\theta) = \text{Tr}(\eta_V \log \rho_V(\theta))$ . Since  $\eta_V$  is diagonal and  $[\eta_V, \rho_V] = 0$ ,  $\rho_V$  is diagonal. Hence, Theorem 5.1 applies.

Since  $\eta_V$  and  $\rho_V$  are diagonal, we expand the log-likelihood into a sum across the dataset  $\mathfrak{D}$

$$\mathcal{L}(\theta) = \frac{1}{N} \sum_{i=1}^N \log P(\mathbf{v}^{(i)} | \theta)$$

giving the required expression.  $\square$

### Proof of Corollary 5.3

**Corollary.** A Hamiltonian-based model  $\rho(\theta) = e^{\mathbf{H}(\theta)} / Z(\theta)$  with  $\mathbf{H}(\theta) = \sum_r \theta_r \mathbf{H}_r$  is a **CQ-LVM** if and only if  $\mathbf{H} = \oplus_i \mathbf{H}_i$  where  $\mathbf{H}_i$  are Hermitian operators in  $\mathfrak{L}(\mathcal{H}_L)$  and  $i \in [2^{d_V}]$ .

*Proof.* The Taylor series of the matrix exponential is given by  $e^X = \sum_{k=0}^{\infty} \frac{1}{k!} X^k$ . Since  $\mathcal{H}$  is a block diagonal matrix, the powers of  $\mathcal{H}$  are also block diagonal. Therefore  $\rho$  is also a block diagonal matrix as required.

Similarly, the Taylor series of the matrix logarithm is given by  $\log X = -\sum_{k=1}^{\infty} \frac{1}{k} (I - X)^k$ . If  $(\log Z)\rho = e^{\mathcal{H}}$  is a block diagonal matrix, then its logarithm  $\mathcal{H}$  is also a block diagonal matrix as required.  $\square$

#### Proof of Lemma 5.4

**Lemma.** For diagonal  $\eta_V$  in  $\mathcal{P}(\mathcal{H}_V)$  and a **CQ-LVM**  $\rho(\theta)$ , the log-likelihood of a data point  $\mathbf{v}^{(i)} \in \mathfrak{D}$ ,  $\ell_i(\theta)$  is lower bounded by

$$\ell_i(\theta) \geq \text{Tr} \left( \eta_L \log(P(\mathbf{v}^{(i)}|\theta) \rho_L^{(i)}(\theta)) \right) - \text{Tr}(\eta_L \log \eta_L)$$

for any density operator  $\eta_L$  in  $\mathcal{P}(\mathcal{H}_L)$  with equality if and only if  $\eta_L = \rho_L^{(i)}(\theta)$ . Hence, the PRM is given by  $\mathcal{R}_\rho(\eta_V) = \oplus_i P_{\mathcal{D}}(V = \mathbf{v}_i) \rho_L(i | \theta)$ .

*Proof.* We first note that  $\rho(\mathbf{v}|\theta)$  is full rank for all  $\mathbf{v}$  and  $\theta$ . Let  $\eta_L$  be an arbitrary density operator on  $\mathcal{P}(\mathcal{H}_L)$ . The Umegaki relative entropy between two density operators is always non-negative when defined.

$$\begin{aligned} D_U(\eta_L, \rho(\mathbf{v}^{(i)}|\theta)) &\geq 0 \\ -S(\eta_L) - \text{Tr}(\eta_L \log(\rho(\mathbf{v}^{(i)}|\theta))) &\geq 0 \\ -\text{Tr} \left( \eta_L \log \left( \frac{P(\mathbf{v}^{(i)}|\theta)}{P(\mathbf{v}^{(i)}|\theta)} \rho(\mathbf{v}^{(i)}|\theta) \right) \right) &\geq S(\eta_L) \\ \text{Tr} \left( \log \left( P(\mathbf{v}^{(i)}|\theta) \right) I_L \right) - \text{Tr} \left( \eta_L \log \left( P(\mathbf{v}^{(i)}|\theta) \rho(\mathbf{v}^{(i)}|\theta) \right) \right) &\geq S(\eta_L) \\ \log \left( P(\mathbf{v}^{(i)}|\theta) \right) &\geq \text{Tr} \left( \eta_L \log \left( P(\mathbf{v}^{(i)}|\theta) \rho(\mathbf{v}^{(i)}|\theta) \right) \right) + S(\eta_L) \\ \ell_{(i)}(\theta) &\geq \text{Tr} \left( \eta_L \log \left( P(\mathbf{v}^{(i)}|\theta) \rho(\mathbf{v}^{(i)}|\theta) \right) \right) + S(\eta_L). \end{aligned}$$

The equality condition is direct since  $D_U(\eta_L, \rho(\mathbf{v}^{(i)}|\theta)) = 0$  if and only if  $\eta_L = \rho(\mathbf{v}^{(i)}|\theta)$ .

The Petz Recovery Map, is immediately obtained by applying **Condition S** to Lemma 5.2.  $\square$

#### Proof of Corollary 5.5

**Corollary.** A  $\text{QBM}_{m,n}$  is a **CQ-LVM** if and only if quantum terms on the visible units are zero.

*Proof.* We recall the Hamiltonian of a  $\text{QBM}_{m,n}$ .

$$H = - \sum_{i=1}^{m+n} b_i \sigma_i^z - \sum_{i>j} w_{ij} \sigma_i^z \sigma_j^z - \sum_{i=1}^{m+n} \Gamma_i \sigma_i^x$$

We first note that Corollary 5.3 implies that the Hamiltonian is CQ if and only if it is a direct sum of  $2^m$  matrices of size  $2^n \times 2^n$ .

The only off-diagonal entries of the Hamiltonian are from the quantum bias terms  $\Gamma_i$ . Recall that  $\sigma_i^x$  are defined as

$$\sigma_i^k = \otimes_{j=1}^{i-1} I \otimes \sigma^k \otimes_{j=i+1}^{m+n} I$$

where  $\sigma^x = \begin{pmatrix} 0 & 1 \\ 1 & 0 \end{pmatrix}$  and  $I = \begin{pmatrix} 1 & 0 \\ 0 & 1 \end{pmatrix}$ . It is easy to see that  $\sigma_i^x = \oplus_{j=1}^i (\sigma^k \otimes_{j=i+1}^{m+n} I)$  for  $i > m$  which satisfies the condition in Corollary 5.3.

To prove the other direction, we observe that the Kronecker product  $\sigma^x \otimes M = \begin{pmatrix} 0 & M \\ M & 0 \end{pmatrix}$  for any square matrix  $M$ . When  $i \leq m$ , this results in matrices larger than  $2^n \times 2^n$  with non-zero entries which cannot then be represented as a direct sum of  $2^n \times 2^n$  matrices. Hence,  $\Gamma_i = 0$  if  $i \leq m$ .  $\square$

#### Justification for Gibbs sampling step

In this subsection, we denote vectors in Hilbert space  $|x\rangle \in \mathcal{H}$ , their adjoint in the dual space  $\langle y| \in \mathcal{H}^*$ , and their inner product  $\langle y|x\rangle \in \mathbb{C}$ . The Z and X basis is the eigenbasis of the  $\sigma_i^z$  and  $\sigma_i^x$  operators respectively. We consider the Ising model with a transverse field only in the hidden layer and establish elementary properties of the Hamiltonian. Below,  $|v\rangle$  is in the Z basis and each component  $|v_i\rangle$ ,  $i \in [m]$  is labeled by its eigenvalue  $v_i = \pm 1$  of the single-spin Pauli operator  $\sigma_i^z$ .

Thus, it corresponds to  $\mathbf{v} \in \{-1, 1\}^m$  in the main text. State vectors in other layers also follow this convention. The index  $k \in [2^m]$  below and  $k = 0$  corresponds to all the spins  $v_i = -1$ .

$$H = \sum_{i,j} w_{ij} \sigma_i^z \sigma_j^z + \sum_i b_i \sigma_i^z + \sum_{j \in L} \Gamma_j \sigma_j^x \quad (3)$$

The data density operator is defined over the visible Hilbert space and is assumed to be diagonal in the Z-basis.

$$\eta_V = \sum_k \alpha_k |v^{(k)}\rangle \langle v^{(k)}| = \sum_{k=1}^{2^m} \alpha_k \Lambda_k \text{ where } \alpha_k \geq 0 \text{ and } \sum_{k \in V} \alpha_k = 1.$$

**Proposition C.2** (Commutation with the Hamiltonian). *Let  $\Lambda_k = |v^{(k)}\rangle \langle v^{(k)}|$  denote a projection operator in the Z-basis of the visible Hilbert space. If the transverse field only appears on the hidden qubits, the following holds*

$$[H, \Lambda_k \otimes I_L] = 0.$$

The Hamiltonian (3) may then be written as

$$H = \sum_k \Lambda_k \otimes \hat{H}_k, \text{ with } \hat{H}_k = \text{Tr}_V[(\Lambda_k \otimes I_L)H].$$

**Definition C.3** (QRBM Model). A model with Hamiltonian of the form 3 is called Quantum Restricted Boltzmann machine if there are no hidden-hidden qubit interactions i.e.,  $w_{ij} = 0$  for all  $i, j \in L$ , and no visible-visible interactions  $w_{ij} = 0$  for all  $i, j \in V$ .

For this model,  $\hat{H}_k$  is

$$\hat{H}_k = E^{(k)} I_L + \sum_{j \in L} b_j^{(k)} \sigma_j^z + \Gamma_j \sigma_j^x. \quad (4)$$

Here  $E^{(k)} = \sum_{i \in V} b_i v_i^{(k)}$  and  $b_j^{(k)} = \sum_{i \in V} w_{ij} v_i^{(k)} + b_j$ . The Hamiltonian 4 is thus non-interacting and is readily diagonalizable. These become independent qubit systems in an external magnetic field given by  $\mathbf{D}_j^{(k)} = (\Gamma_j, 0, b_j^{(k)})$ . We shall denote the magnitude of the field by  $|\mathbf{D}_j^{(k)}| = \sqrt{(b_j^{(k)})^2 + \Gamma_j^2}$ . Each qubit system has eigenvalues  $E^{(k)} \pm |\mathbf{D}_j^{(k)}|$ . Dropping the constant  $E^{(k)}$ , expected values can be calculated using the partition function  $Z_j = 2 \cosh |\mathbf{D}_j^{(k)}|$ . If we have the visible layer clamped to a vector  $|\mathbf{v}\rangle = |v^{(k)}\rangle$ , the expected values of the spins  $j \in L$  in the hidden layer are

$$\begin{aligned} \langle \sigma_j^z \rangle &= \frac{b_j^{(k)}}{|\mathbf{D}_j^{(k)}|} \tanh |\mathbf{D}_j^{(k)}| \\ \langle \sigma_j^x \rangle &= \frac{\Gamma_j}{|\mathbf{D}_j^{(k)}|} \tanh |\mathbf{D}_j^{(k)}| \end{aligned} \quad (5)$$

Similarly, in a QiDBM, the total Hamiltonian  $[H, \Lambda_{k,V} \otimes I_{L^{(1)}} \otimes \Lambda_{k',L^{(2)}}] = 0$  for projection operators taken in the Z basis. If we clamp the visible layer to  $\mathbf{v} = \mathbf{v}^{(k)}$  and the second hidden layer to  $\mathbf{h}^{(2)} = \mathbf{h}^{(2)(k')}$ , the resulting Hamiltonian

$$\hat{H}_{k,k'} = E^{(k,k')} I_{L^{(1)}} + \sum_{j \in L^{(1)}} b_j^{(k,k')} \sigma_j^z + \Gamma_j \sigma_j^x,$$

which is again non-interacting and readily diagonalizable.  $E^{(k,k')} = \sum_{i \in V} b_i v_i^{(k)} + \sum_{i' \in L^{(2)}} b_{i'} h_{i'}^{(2)(k')}$  and the biases in the first hidden layer  $j \in L^{(1)}$  are  $b_j^{(k,k')} = \sum_{i \in V} w_{ij}^{(1)} v_i^{(k)} + \sum_{i' \in L^{(2)}} w_{ij}^{(2)} h_{i'}^{(2)(k')} + b_j$ . With these, the external fields are now  $\mathbf{D}^{(k,k')} = (\Gamma_j, 0, b_j^{(k,k')})$  and the expected values are again given by (5). The conditional probabilities for sampling in the Z and X basis are again given by

$$\begin{aligned} P(h_j^{(1)z} = 1 | \mathbf{v} = \mathbf{v}^{(k)}, \mathbf{h}^{(2)} = \mathbf{h}^{(2)(k')}) &= \frac{1 + \langle \sigma_j^z \rangle}{2}, \\ P(h_j^{(1)x} = 1 | \mathbf{v} = \mathbf{v}^{(k)}, \mathbf{h}^{(2)} = \mathbf{h}^{(2)(k')}) &= \frac{1 + \langle \sigma_j^x \rangle}{2}. \end{aligned}$$

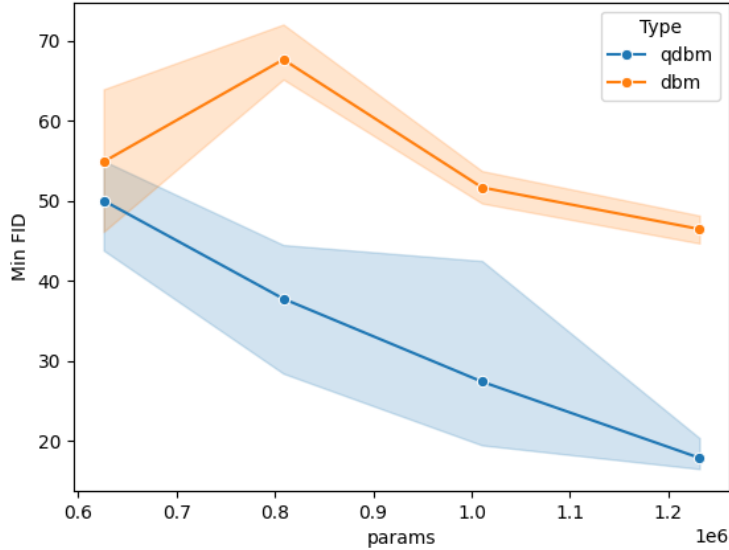


Figure 2: FID vs Parameters of QiDBM and DBM on Binarized MNIST with error bars.

## D Experimental details and Additional Experiments

### D.1 Additional Experiments

In this section, we restate key details of our experiments presented in the main body of this work. In the interest of keeping this section self-contained, we restate our experimental setup. Following the implementation of [22], we use  $\{0, 1\}$  encoding instead of  $\{-1, 1\}$ .

To compare the effect of the addition of quantum bias, we compare the performance of trained models with and without quantum bias across different sizes. We train a QiDBM and DBM on 1 bit MNIST with hidden sizes 498, 588, 686, and 784 for 100 epochs with 2 hidden layers with SGD optimized to perform Contrastive Divergence with a batch size of 600. In Figure 1 (c), we plot the number of parameters with the minimum FID obtained over 100 epochs. We observe that the model with quantum bias clearly outperforms the models without quantum bias. We also observe that the QiDBM obtains similar FID scores with much fewer parameters than the DBM. In Figure 2, we provide the same plot with 3 different random seeds. We continue to observe that the QiDBM outperforms the DBM.

In Figure 3, we show generated images from different stages of training between QiDBMs and DBMs trained on 8 bit MNIST at randomly selected checkpoints. We observe that the QiDBM produces better quality images in earlier stages of training.

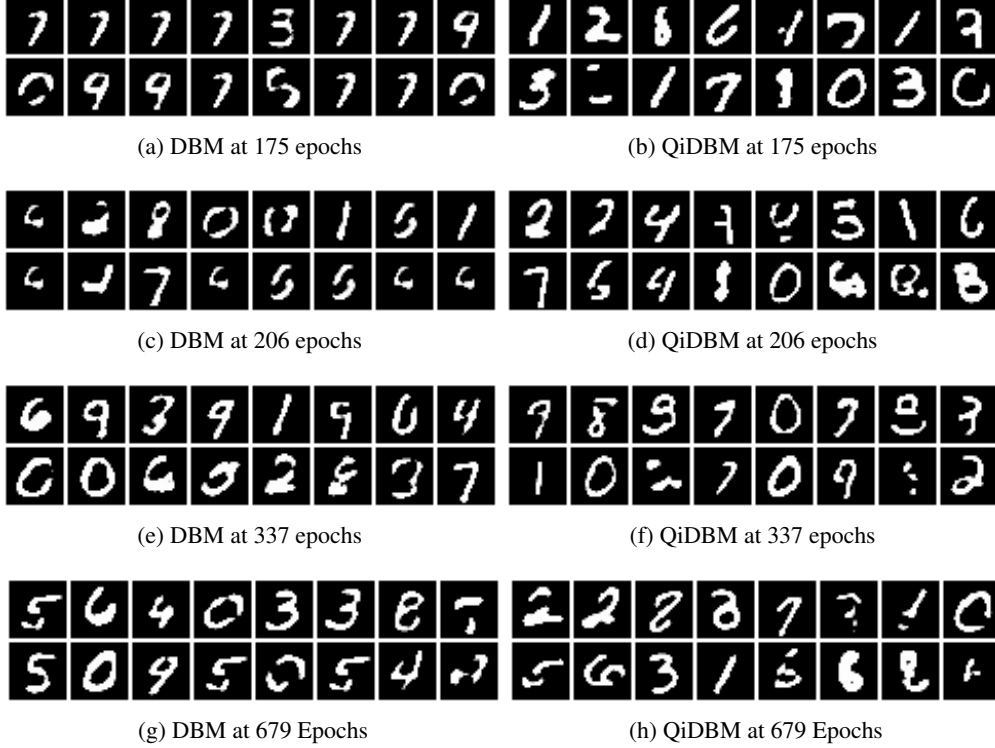


Figure 3: Generated samples during training. DBM generated images on the Left and QiDBM generated images on the Right

## D.2 Mixture of Bernoulli Dataset

We describe the dataset from Amin et al. [12] used in our experiments to showcase the practicality of our proposed method. A Bernoulli distribution is built on a randomly selected mode and the average probability distribution over  $M$  such modes determines the mixture of Bernoulli distribution. The distribution can be written as

$$P_v^{\text{data}} = \frac{1}{M} \sum_{k=1}^M p^{N-d_v^k} (1-p)^{d_v^k} \quad (6)$$

where  $N$  is the dimension of data,  $p$  is the probability of success, and  $d_v^k$  is the Hamming distance between  $v$  and the randomly selected mode. We use 100 randomly sampled datasets of 1000 samples each with  $N = 1000$ ,  $M = 8$ ,  $N = 8$ , and  $p = 0.9$ .

## E Compute Platform

**Implementation Details** We implement our proposed methods in PyTorch 2.5.1.

**Hardware** Tables 1 and 2 details the hardware we use to conduct our experiments. Values in (\*) indicated reported values obtained from <https://www.amd.com/en/products/accelerators/instinct/mi200/mi210.html>. Machine 1 runs Ubuntu 22.04.3 LTS with kernel 6.8.0-40-generic with the hardware in Table 1. Machine 2 runs Ubuntu 22.04.1 LTS with kernel 5.15.0-127-generic with the hardware in Table 2. Our software stack comprises of 3.12.8, PyTorch 2.5.1, torchvision version 0.20.1.

Table 1: Machine 1: Specifications of GPU hardware used for computation

CPU Model Name	AMD EPYC 9654 96-Core Processor
CPU(s)	192
Thread(s) per core	1
Core(s) per socket	96
Socket(s)	2
NUMA node(s)	2
CPU MHz(Max)	3707.8120
L1d & L1i cache	6 MiB
L2 cache	192 MiB
L3 cache	768 MiB
RAM	1.48 TiB (DDR5, 4800 MT/s)
GPU Model name	Instinct MI210
GPU(s)	4
GPU Architecture	AMD Aldebaran
Dedicated Memory Size(per GPU)	64 GB
ROCm Version	6.0.2
Peak FP32 Performance*	22.6 TFLOPs
Peak FP64 Performance*	22.6 TFLOPs
Memory Clock*	1.6 GHz
Peak Memory Bandwidth*	1.6 TB/s

Table 2: Machine 2: Specifications of GPU hardware used for computation

CPU Model Name	Intel(R) Core(TM) i9-10980XE
CPU(s)	36
Thread(s) per core	2
Core(s) per socket	18
Socket(s)	1
NUMA node(s)	1
CPU MHz(Max)	4800.0000
L1d & L1i cache	576 KiB
L2 cache	18 MiB
L3 cache	24.8 MiB
RAM	125GiB
GPU Model name	NVIDIA GeForce RTX 3090
GPU(s)	2
Dedicated Memory Size(per GPU)	24 GB
CUDA Version	12.2

## F Limitations

This work only addresses finite dimensional Hilbert spaces, analogues of discrete probability spaces. While most of the results in this work generalize to the continuous case, we leave their analysis for future work. Although the DO EM algorithm is amenable to implementation on a quantum computer, as discussed in Section 7, its precise design and analysis needs further research.